THE JOURNAL OF PHYSICAL CHEMISTRY A

Article

Cite This: J. Phys. Chem. A 2019, 123, 1110−1128

pubs.acs.org/JPCA

Surface Hopping without Momentum Jumps: A Quantum-Trajectory-Based Approach to Nonadiabatic Dynamics

Published as part of The Journal of Physical Chemistry virtual special issue "William P. Reinhardt Festschrift".

Craig C. Martens*

University of California, Irvine, California 92697-2025, United States

ABSTRACT: We describe a new method for simulating nonadiabatic dynamics using stochastic trajectories. The method, which we call quantum trajectory surface hopping (QTSH), is a variant of the popular fewest-switches surface-hopping (FSSH) approach, but with important differences. We briefly review and significantly extend our recently described consensus surface-hopping (CSH) formalism, which captures quantum effects such as coherence and decoherence via a collective representation of the quantum dynamics at the ensemble level. Using well-controlled further approximations, we derive an independent trajectory limit of CSH that recovers the FSSH stochastic algorithm but rejects the ad hoc momentum rescaling of FSSH in favor of quantum forces that couple classical and quantum degrees of freedom and lead to nonclassical trajectory dynamics. The approach is well-defined in both the diabatic and adiabatic representations. In the adiabatic representation, the classical dynamics are modified by a quantum-state-dependent vector potential, introducing geometric phase effects into the dynamics of multidimensional systems. Unlike FSSH, our method obeys energy conservation without any artificial momentum rescaling, eliminating undesirable features of the former such as forbidden hops and breakdown of the internal consistency of quantum and ensemble-based state probabilities. Corrections emerge naturally in the formalism that allow approximate incorporation of decoherence without the computational expense of the full CSH approach. The method is tested on several model systems. QTSH provides a surface-hopping methodology that has a rigorous foundation and broader applicability than FSSH while retaining the low computational cost of an independent trajectory framework.

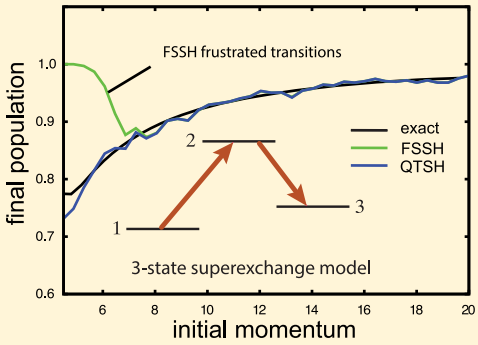

1. INTRODUCTION

Trajectory surface hopping is a popular and efficient method for simulating the coupled electronic and nuclear dynamics of molecular systems in a quantum-classical framework.[1−11] The most commonly used implementation is the fewest-switches surface-hopping (FSSH) method, originally introduced by Tully in 1990,[1] and its many subsequent variants (see, e.g., refs 9−11 for reviews). In the FSSH approach, the evolving multicomponent nuclear quantum wavepacket is approximated by an ensemble of independent classical trajectories, each of which carries its own copy of an electronic Schrödinger equation that evolves under the influence of the time-dependent classical variables and determines the probability of sudden stochastic transitions of the trajectory between the quantum states. FSSH has proven to be a simple and robust method for simulating classical molecular dynamics with quantum electronic transitions.

The FSSH method has a number of well-known shortcomings that limit its applicability. In particular, the original implementation does not treat quantum coherence, and especially decoherence, properly, leading to a representation of the quantum evolution that is overcoherent, in the sense that the off-diagonal quantum density matrix elements of individual trajectories can be spuriously large in magnitude compared with the exact quantum coherence. Attempts to improve FSSH have mainly focused on corrections to this problem. Another issue is related to the strict classical energy conservation imposed on the individual trajectories in FSSH. When a trajectory undergoes a transition between electronic states, the corresponding difference in electronic-state energies at the transition point is accommodated in the nuclear dynamics by an ad hoc rescaling of the momentum along the nonadiabatic coupling vector. This algorithm, although quite physically reasonable prima facie, has no rigorous foundation based on first principles. The FSSH algorithm also results in practical problems, such as the spurious closing of classically forbidden channels allowed by the full quantum evolution and the presence of "frustrated hops", transitions that are dictated to occur by the surface-hopping stochastic process but rejected by the ad hoc imposition of classical energy conservation. These events break the consistency of surface hopping—the agreement between the evolving quantum density matrix probabilities and the state populations reflected by the hopping trajectory ensemble. Furthermore, the use of the nonadiabatic coupling vector in the momentum rescaling is only well-defined in the adiabatic representation of electronic states,

Received: October 28, 2018
Revised: January 11, 2019
Published: January 11, 2019

DOI: 10.1021/acs.jpca.8b10487
J. Phys. Chem. A 2019, 123, 1110−1128

limiting the applicability of FSSH to dynamics in the adiabatic representation.

Recently, we proposed an alternative surface-hopping framework, consensus surface hopping (CSH),[12] which avoids the independent trajectory approximation and more rigorously incorporates the nonclassical effects of nonlocality, uncertainty, and quantum coherence.[13] The advantages of CSH come at a cost, however, and the method is numerically more expensive than FSSH due to the interdependence of the trajectories in the ensemble. Its use as a computational approach is thus limited to low-dimensional model systems. The greatest value of the CSH formalism, in our opinion, is not as a numerical method for simulations but as a framework for developing additional approximations and more economical methodology in a well-controlled and rigorous manner.

In this Article, we describe such an approximate approach, quantum trajectory surface hopping (QTSH). The theory develops from a rigorous quantum-classical limit of the multistate quantum Liouville equation[14−20] in the context of the computationally efficient independent trajectory-based FSSH method. We take an approximate independent trajectory limit of the full CSH method, yielding an algorithm that is equivalent to the standard FSSH stochastic trajectory hopping approach. The main difference with FSSH is the abandonment of ad hoc momentum rescaling to conserve the classical kinetic-plus-potential energy at the individual trajectory level and its replacement by quantum forces derived rigorously from the semiclassical-limit quantum-classical Liouville equation. This feature of the method restores the consistency of surface hopping that is broken by the frustrated hops of the standard FSSH approach. In addition, the energetics of the system are treated correctly: The full quantum-classical energy is conserved rigorously at the ensemble level. The ensemble average energy conservation is the correct behavior required by quantum mechanics; individual trajectory conservation of the classical energy is a constraint that is too restrictive and too classical and so precludes important quantum effects. Further corrections are developed and implemented to incorporate average ensemble-level decoherence as an approximation to the full CSH treatment of coherence. The approach is tested on standard 1D models. For cases where FSSH works well, the QTSH approach gives similar results for an equivalent computational cost. In situations where FSSH fails due to spuriously frustrated hops, the QTSH method continues to give results in close agreement with quantum mechanics.

The organization of the rest of this paper is as follows. In Section 2, we review the standard FSSH methodology. We then briefly summarize the full CSH approach as reported previously[13] and significantly extend its treatment of energy conservation through electronic-state-dependent nonclassical forces. The QTSH approach, the quantum trajectory modification of FSSH, is developed in both the diabatic and adiabatic representations. Numerical results comparing the methods for a number of model systems are presented in Section 3. Finally, a summary and discussion is given in Section 4.

2. THEORY

2.1. Fewest-Switches Surface Hopping. We begin by briefly reviewing the FSSH method proposed by Tully in 1990.[1] The total Hamiltonian describing the electronic and nuclear degrees of a molecular system is given by

$$\hat{H} = \hat{T}_{\mathbf{q}} + \hat{H}_{\mathrm{o}}(\mathbf{r}, \mathbf{q}) \tag{1}$$

Here $\mathbf{r}$ and $\mathbf{q}$ are the electronic and nuclear coordinates, respectively. $\hat{T}_{\mathbf{q}}$ is the nuclear kinetic energy, whereas $\hat{H}_{\mathrm{o}}(\mathbf{r},\mathbf{q})$ is the electronic Hamiltonian, which depends parametrically on the nuclear coordinates $\mathbf{q}$. An electronic basis is chosen in terms of states $\phi_n(\mathbf{r};\mathbf{q})$, which are functions of the electronic coordinates $\mathbf{r}$ and may also depend parametrically on the nuclear coordinates $\mathbf{q}$. Matrix elements of the electronic Hamiltonian are given by

$$V_{mn}(\mathbf{q}) = \int \phi_m^*(\mathbf{r};\, \mathbf{q}) \hat{H}_{\mathrm{o}}(\mathbf{r},\, \mathbf{q}) \phi_n(\mathbf{r};\, \mathbf{q})\, \mathrm{d}\mathbf{r} \tag{2}$$

In the adiabatic representation, the electronic wave functions depend on $\mathbf{q}$, and the derivative coupling matrix element $\mathbf{d}_{mn}(\mathbf{q})$ results from off-diagonal matrix elements of the nuclear kinetic energy

$$\mathbf{d}_{mn}(\mathbf{q}) = \int \phi_m^*(\mathbf{r};\, \mathbf{q}) \nabla_{\mathbf{q}} \phi_n(\mathbf{r};\, \mathbf{q})\, \mathrm{d}\mathbf{r} \tag{3}$$

The FSSH formalism approaches the problem of nonadiabatic dynamics by using classical trajectories and ensemble averaging to approximate the nuclear quantum dynamics of a multicomponent wavepacket. These classical trajectories capture the quantum electronic transitions by stochastic "hops" between the electronic surfaces. The electronic degrees of freedom are, in turn, driven by the time-dependent nuclear trajectories $\mathbf{q}(t)$ that appear in the nuclear coordinate dependence of the electronic Hamiltonian. For a given classical path $\mathbf{q}(t)$, the electronic wave function can be expanded in the chosen electronic basis as

$$\psi(\mathrm{r},\, t) = \sum_n c_n(t) \phi_j(\mathbf{r};\, \mathbf{q}(\mathbf{t})) \tag{4}$$

The substitution of this expression into the time-dependent Schrödinger equation yields a set of coupled equations for the expansion coefficients

$$i\hbar \dot{c}_m(t) = \sum_n (V_{mn} - i\hbar \dot{\mathbf{q}} \cdot \mathbf{d}_{mn}) c_n(t) \tag{5}$$

It is convenient to use the quantum density matrix, $a_{mn} = c_m c_n^*$, rather than the wave function amplitudes, c_m. The quantum equations of motion then become

$$i\hbar \dot{a}_{mn}(t) = \sum_l [(V_{ml} - i\hbar \dot{\mathbf{q}} \cdot \mathbf{d}_{ml}) a_{ln} - a_{ml}(V_{ln} - i\hbar \dot{\mathbf{q}} \cdot \mathbf{d}_{ln})] \tag{6}$$

Here the following relations hold

$$\mathbf{d}_{ln}^* = -\mathbf{d}_{nl} \tag{7}$$

$$\mathbf{d}_{nn}^* = 0 \tag{8}$$

The equation of motion for the population of the nth state, represented by the diagonal density matrix element, a_{nn}, is then given by

$$\dot{a}_{nn} = \sum_{l \neq n} b_{nl} \tag{9}$$

where

$$b_{nl} = \frac{2}{\hbar} \mathrm{Im}(a_{nl}^* V_{nl}) - 2\mathrm{Re}(a_{nl}^* \dot{\mathbf{q}} \cdot \mathbf{d}_{nl}) \tag{10}$$

DOI: 10.1021/acs.jpca.8b10487
J. Phys. Chem. A 2019, 123, 1110−1128

It should be remembered that $V_{nl}(\mathbf{q}(t))$ and $\mathbf{d}_{nl}(\mathbf{q}(t))$ as well as $\dot{\mathbf{q}}(t)$ all depend on the time-dependent classical path, $\mathbf{q}(t)$.

In the FSSH method, an ensemble of independent trajectories $(\mathbf{q}_j(t),\mathbf{p}_j(t))$ (j = 1, 2, ..., N) is sampled from a distribution representing the initial nuclear quantum state, where $\mathbf{p}_j$ is the canonical momentum conjugate to the jth trajectory's nuclear coordinate $\mathbf{q}_j$. Each trajectory so generated is initiated on one of the electronic states and then evolves under Hamilton's equations that correspond to the instantaneous occupied state. Stochastic transitions occur between these states with a probability that is proportional to the relative rate of change of the quantum populations associated with the trajectory.

To illustrate, we consider a system with two electronic states and a trajectory currently evolving on state 1 (here we suppress the trajectory index j). In the FSSH method, this trajectory has a probability of hopping from surface 1 to surface 2 if $\dot{a}_{11}(t)$ is negative. In that case, $P_{\text{hop}}^{\text{FSSH}}(t)$, the probability of hopping at time t during a time step of duration Δt, is then given by

$$P_{\text{hop}}^{\text{FSSH}}(t) = \left| \frac{1}{a_{11}(t)} b_{12}(t) \Delta t \right| \tag{11}$$

The hop is realized or not by generating a random number between 0 and 1 and comparing it with $P_{\text{hop}}^{\text{FSSH}}(t)$. An analogous procedure is used for trajectories currently on state 2.

Strict energy conservation at the individual trajectory level is imposed by rescaling the momenta at the instant of the hop so that the total kinetic plus potential energy of the trajectory remains unchanged during the transition. In multidimensional systems, the momentum rescaling is performed along the direction of the nonadiabatic coupling vector, $\mathbf{d}_{12}$. If insufficient energy is available for an upward hop in energy, then the event is termed "frustrated" and does not occur despite the stochastic algorithm dictating the transition. Such aborted events lead to a breakdown of the consistency between the density matrix populations and the trajectory ensemble statistics.

2.2. Consensus Surface Hopping. The FSSH method is a sensible but ad hoc solution to the problem of modeling nonadiabatic dynamics with trajectories. The algorithm was proposed based on physical reasoning rather than derived systematically from the underlying exact quantum dynamics. The CSH approach seeks to go beyond this and build a trajectory-based method for nonadiabatic dynamics simulations with a rigorous foundation.[12] The CSH formalism focuses on solving the multistate quantum Liouville equation for coupled electronic and nuclear dynamics in the semiclassical limit using trajectory ensembles to represent phase-space densities.[14−18] These states evolve quantum mechanically, and so the trajectory dynamics must correspondingly become nonclassical.

An initial description of the approach was given in ref 12. Here we provide a review of that work and, in addition, significantly extend the formalism to give a more rigorous treatment of the energy conservation by the inclusion of nonclassical terms in the phase-space dynamics. This additional aspect will be a key component of the QTSH approach that is the focus of this paper and is developed below.

The quantum-mechanical Liouville equation for the density operator $\hat{\rho}(t)$ is given by[21]

$$i\hbar \frac{\mathrm{d}\hat{\rho}(t)}{\mathrm{d}t} = [\hat{H}, \hat{\rho}(t)] \tag{12}$$

where $\hat{H}$ is the Hamiltonian of the system. For dynamics on a single potential surface, the classical limit of eq 12 is the well-known classical Liouville equation of nonequilibrium statistical mechanics[22]

$$\frac{\partial \rho}{\partial t} = \{H, \rho\} \tag{13}$$

where $\rho(\mathbf{q},\mathbf{p},t)$ and $H(\mathbf{q},\mathbf{p},t)$ are now functions of the $2f$-dimensional (for f nuclear degrees of freedom) phase-space variables $\Gamma = (\mathbf{q},\mathbf{p})$ and time t, and $\{H,\rho\}$ is the Poisson bracket of H and ρ: $\{H,\rho\} = \partial H/\partial \mathbf{q}\cdot\partial\rho/\partial\mathbf{p} - \partial\rho/\partial\mathbf{q}\cdot\partial H/\partial\mathbf{p}$. This correspondence can be derived systematically from eq 12 by performing a Wigner−Moyal expansion[23,24] of the quantum-mechanical Liouville equation. To lowest order in $\hbar$, this involves replacing commutators by Poisson brackets: $[\hat{A},\hat{B}] \rightarrow i\hbar\{A,B\} + O(\hbar^2)$.

Diabatic Representation. The semiclassical limit of eq 12 can be generalized to two coupled quantum states coupled to classical degrees of freedom. The approach is general for mixed quantum-classical problems. Here we consider two quantum electronic states in the diabatic electronic representation coupled to classical limit nuclear dynamics. The Hamiltonian and density matrix are given by 2 × 2 matrices

$$\hat{H} = \begin{pmatrix} \hat{H}_{11} & \hat{V} \\ \hat{V} & \hat{H}_{22} \end{pmatrix} \tag{14}$$

and

$$\hat{\rho}(t) = \begin{pmatrix} \hat{\rho}_{11}(t) & \hat{\rho}_{12}(t) \\ \hat{\rho}_{21}(t) & \hat{\rho}_{22}(t) \end{pmatrix} \tag{15}$$

respectively. The elements of these matrices are nuclear operators. With the replacement of the quantum-mechanical operators by the corresponding classical phase-space functions, this becomes a set of coupled classical-like Liouville equations[14−18,25−30]

$$\frac{\partial \rho_{11}}{\partial t} = \{H_{11}, \rho_{11}\} + \{V, \alpha\} - \frac{2V}{\hbar}\beta \tag{16}$$

$$\frac{\partial \rho_{22}}{\partial t} = \{H_{22}, \rho_{22}\} + \{V, \alpha\} + \frac{2V}{\hbar}\beta \tag{17}$$

$$\frac{\partial \alpha}{\partial t} = \{H_0, \alpha\} + \omega\beta + \frac{1}{2}\{V, \rho_{11} + \rho_{22}\} \tag{18}$$

$$\frac{\partial \beta}{\partial t} = \{H_0, \beta\} - \omega\alpha + \frac{V}{\hbar}(\rho_{11} - \rho_{22}) \tag{19}$$

Here we have written the coherence $\rho_{12}(\Gamma,t) = \alpha(\Gamma,t) + i\beta(\Gamma,t)$ in terms of its real and imaginary parts and have defined the average Hamiltonian $H_0 = (H_{11} + H_{22})/2$ and the frequency $\omega = (H_{11} - H_{22})/\hbar$. All higher order terms in $\hbar$ have been neglected, leading to a classical-limit formalism that retains only the most important nonclassical corrections.

The CSH method employs a trajectory ensemble representation of the phase-space functions describing the density matrix in the coupled semiclassical Liouville equations. Quantum population transfer is represented by stochastic trajectory hops between the diagonal surfaces, whereas

DOI: 10.1021/acs.jpca.8b10487
J. Phys. Chem. A 2019, 123, 1110−1128

quantum coherence is represented collectively at the ensemble level by interrelationships between nonclassical amplitudes and phases associated with each trajectory.

The phase-space densities corresponding to the populations of states 1 and 2 are together represented by a single ensemble of N trajectories, each of which is characterized by a point in phase space $\Gamma_j(t) = (\mathbf{q}_j(t),\mathbf{p}_j(t))$ and a binary integer $\sigma_j(t)$, which can take on the values 1 or 0, indicating whether the trajectory is associated with quantum state 1 or 2, respectively. The states 1 and 2 phase-space densities are then given by

$$\rho_{11}(\Gamma, t) = \frac{1}{N}\sum_{j=1}^{N} \sigma_j(t)\delta(\Gamma - \Gamma_j(t)) \tag{20}$$

and

$$\rho_{22}(\Gamma, t) = \frac{1}{N}\sum_{j=1}^{N} (1 - \sigma_j(t))\delta(\Gamma - \Gamma_j(t)) \tag{21}$$

respectively. The δ functions represent the discrete points of the trajectories in phase space, whereas the coefficients σ_j denote which state the trajectory currently occupies. In the numerical implementation involving finite trajectory ensembles, the δ functions are smoothed using phase-space Gaussians, as described in ref 12. This results in the replacement of the delta functions by the Gaussian basis $g(\Gamma)$: $\delta(\Gamma - \Gamma_j) \rightarrow g(\Gamma - \Gamma_j)$.

The coherence $\rho_{12}(\Gamma,t)$ is also represented in terms of the trajectory ensemble. Unlike the populations, however, the coherence is a complex quantity, and thus the coefficients of the trajectories are complex numbers. The populations and the real and imaginary parts of the coherence are given in terms of the smoothed trajectory ensemble as

$$\rho_{11}(\Gamma, t) = \frac{1}{N}\sum_{j=1}^{N} \sigma_j(t)g(\Gamma - \Gamma_j(t)) \tag{22}$$

$$\rho_{22}(\Gamma, t) = \frac{1}{N}\sum_{j=1}^{N} (1 - \sigma_j(t))g(\Gamma - \Gamma_j(t)) \tag{23}$$

$$\alpha(\Gamma, t) = \frac{1}{N}\sum_{j=1}^{N} \alpha_j(t)g(\Gamma - \Gamma_j(t)) \tag{24}$$

$$\beta(\Gamma, t) = \frac{1}{N}\sum_{j=1}^{N} \beta_j(t)g(\Gamma - \Gamma_j(t)) \tag{25}$$

The coefficients $\sigma_j(t)$ are stochastic binary integers, whereas $\alpha_j(t)$ and $\beta_j(t)$ (j = 1, 2, ..., N) are continuous real numbers. (We note that it is not necessary to make such a distinction; in a recent paper, we describe an alternative approach to the general problem of quantum-state hopping that represents both populations and coherence in terms of separate stochastic processes.[31])

The equations of motion for the trajectories, $\Gamma_j(t)$, and state parameters, $(\sigma_j(t), \alpha_j(t), \beta_j(t))$ (j = 1, 2, ..., N), are determined by substituting the trajectory representations, eqs 22−25, into the semiclassical Liouville eqs 16−19. In the uncoupled (V = 0) case, the evolution of the populations reduces to purely classical Liouvillian dynamics corresponding to trajectory ensemble evolution under the appropriate electronic-state Hamiltonian. In the presence of coupling, two types of nonclassical terms appear. The first are sink and source terms $\pm 2V\beta/\hbar$, which are responsible for the population transfer between states. The second type of nonclassical term is the Poisson brackets $\{V,\alpha\}$, which appear symmetrically in the equations for both ρ_{11} and ρ_{22}. These interactions modify the shape of the evolving distributions but do not change the total state populations. Conservation of population under these terms results from the fact that the classical trace (integral over phase-space volume) of a Poisson bracket vanishes for functions satisfying appropriate boundary conditions.

The evolution of the dynamical variables is determined by numerically integrating the ordinary differential equations for the trajectories and the coefficients. Each time step of duration Δt is divided into two parts. First, the coefficients are updated; then, the phase-space trajectories are propagated forward in time.

We first consider the population sink and source terms responsible for the evolution of the stochastic variables $\sigma_j(t)$. To derive a probabilistic algorithm for updating the former we consider the subsets of trajectories on surfaces 1 and 2 separately. For surface 1, substitution into the semiclassical Liouville equations yields

$$\frac{1}{N}\sum_{k=1}^{N} \sigma_k\Delta\sigma_k g(\Gamma - \Gamma_k) = -\frac{1}{N}\sum_{k=1}^{N} \frac{2V(\Gamma)}{\hbar}\beta_k g(\Gamma - \Gamma_k)\Delta t \tag{26}$$

with a similar expression for surface 2. We can evaluate the left and right sides of these expressions at each of the trajectory points of interest, Γ_j, yielding coupled linear equations for the change in coefficients. This gives, for the surface 1 coefficients

$$\frac{1}{N}\sum_{k=1}^{N} \sigma_k\Delta\sigma_k g(\Gamma_j - \Gamma_k) = -\frac{1}{N}\sum_{k=1}^{N} \frac{2V(\Gamma_j)}{\hbar}\beta_k g(\Gamma_j - \Gamma_k)\Delta t \tag{27}$$

for j = 1, 2, ..., N. In general, this presents a linear algebra problem for the determination of the $\Delta\sigma_j$. We can simplify its solution by making the following approximation that becomes exact as N becomes infinite and the Gaussian functions, $g(\Gamma)$, become localized

$$\frac{1}{N}\sum_{k=1}^{N} \sigma_k\Delta\sigma_k g(\Gamma_j - \Gamma_k) \simeq \langle\rho_{11}\rangle_j\Delta\sigma_j \tag{28}$$

where $\langle\rho_{11}\rangle_j$, the local density at point Γ_j on surface 1, is given by

$$\langle\rho_{11}\rangle_j = \frac{1}{N}\sum_{k=1}^{N} \sigma_k g(\Gamma_j - \Gamma_k) \tag{29}$$

Similarly, we evaluate the value of the coherence at point j as

$$\langle\beta\rangle_j = \frac{1}{N}\sum_{k=1}^{N} \beta_k g(\Gamma_j - \Gamma_k) \tag{30}$$

The equation for updating the coefficients of trajectories currently on surface 1 becomes

$$\Delta\sigma_j = -\frac{1}{\langle\rho_{11}\rangle_j}\frac{2V(\Gamma_j)}{\hbar}\langle\beta\rangle_j\Delta t \tag{31}$$

For trajectories currently evolving on surface 2, the corresponding result is

DOI: 10.1021/acs.jpca.8b10487
J. Phys. Chem. A 2019, 123, 1110−1128

$$\Delta\sigma_j = -\frac{1}{\langle\rho_{22}\rangle_j}\frac{2V(\Gamma_j)}{\hbar}\langle\beta\rangle_j\Delta t \tag{32}$$

These are then identified as the hopping probabilities for the trajectories in the ensemble. For instance, for the jth trajectory currently evolving on state 1, if $\Delta\sigma_j(t)$ is negative, then the trajectory has a nonzero probability of undergoing a hop to state 2 during the time step Δt. The CSH probability for this event is

$$P_{\text{hop}}^{\text{CSH}} = \left|\frac{2}{\hbar\langle\rho_{11}\rangle_j}V(\Gamma_j)\langle\beta\rangle_j\Delta t\right| \tag{33}$$

These equations form the basis of a stochastic hopping algorithm. A random number ξ between 0 and 1 is generated for each trajectory at each time step and compared with the appropriate value of $P_{\text{hop}}^{\text{CSH}} = |\Delta\sigma_j|$ corresponding to the occupied state. The value of $\sigma_j(t)$ is changed by ±1 or kept at its current value depending on the outcome.

The result in eq 33 is strongly reminiscent of the FSSH hopping probability given in eq 11. But we emphasize the essential difference between this approach and the FSSH method. Here the ensemble collectively determines the stochastic hopping probabilities of each of its members. The local densities $\langle\rho_{11}\rangle_j$ and $\langle\rho_{22}\rangle_j$ and the coherence $\langle\beta\rangle_j$ at point Γ_j depend on the ensemble of evolving trajectories $\Gamma_k(t)$ (k = 1, 2, ..., N). They are not independent dynamical variables associated with independent trajectories, as in the FSSH formalism. Quantum transitions are thus determined by a "consensus" among the members of the ensemble representing the full entangled electronic-nuclear quantum state rather than by the independent trajectories of FSSH.

The electronic coherence evolves in parallel with, and coupled to, the evolving population densities. A similar analysis that includes the approximate neglect of terms in eqs 18 and 19 that leave the trace of ρ_{12} unchanged yields expressions that describe the evolution of the coefficients over the time step Δt.[12] Because these equations are solved deterministically rather than by a stochastic hopping algorithm, the limit $\Delta t \to 0$ can be taken, yielding the coupled differential equations

$$\dot{\alpha}_j = \omega(\Gamma_j)\beta_j \tag{34}$$

$$\dot{\beta}_j = \left[-\omega(\Gamma_j)\alpha_j + \frac{1}{\hbar}V(\Gamma_j)(2\sigma_j - 1)\right] \tag{35}$$

These differential equations are integrated numerically using standard methods.

The CSH equations for the coherences are identical to the FSSH density matrix equations for coherences in the diabatic representation if we identify the CSH parameters α_j and β_j with the real and imaginary parts of the jth independent trajectory coherence in the FSSH method.

We emphasize that no artificial decoherence is added to the evolving system in the CSH formalism. The role played by coherence and its decay is treated accurately through the collective nature of the method, as highlighted by eq 30. In particular, decoherence is represented naturally via the cancellation of the signed terms β_k in the summation over Γ_k in the local vicinity of the hopping trajectory, j, to yield $\langle\beta\rangle_j$. If these terms exhibit destructive interference due to either the nature of the pure-state evolution of the multicomponent nuclear wavepacket or by environmental fluctuations in difference potential, $\omega(\Gamma_k)$, over the ensemble, then this summation will be "decayed" by decoherence. The individual β_k values may be quite large; it is only the weighted sum of their values, $\langle\beta\rangle_j$, that becomes small with decoherence. In contrast, FSSH determines hopping probabilities by using the independent individual values of each trajectory's quantum density matrix. This difference is the origin of the over-coherence problem of FSSH.

The rest of this section describes further developments of the CSH formalism that were not included in our previous publication.[12]

We now consider the terms in the evolution equations that involve trace-preserving Poisson brackets. These include both the homogeneous classical phase-space evolution terms of the form $\{H,\rho\}$ and the inhomogeneous nonclassical terms $\{V,\alpha\}$ coupling the density matrix elements.

It is convenient to consider the total nuclear density $\rho = \rho_{11} + \rho_{22}$

$$\rho(\mathbf{q}, \mathbf{p}, t) = \rho_{11}(\mathbf{q}, \mathbf{p}, t) + \rho_{22}(\mathbf{q}, \mathbf{p}, t) = \frac{1}{N}\sum_{j=1}^{N} g(\Gamma - \Gamma_j(t)) \tag{36}$$

This quantity is independent of the stochastic parameters $\sigma_j(t)$ (j = 1, 2, ..., N) (although we will see below that its evolution depends on the quantum-state parameters). The total nuclear density $\rho(\mathbf{q},\mathbf{p},t)$ obeys the partial differential equation obtained by adding eqs 16 and 17

$$\frac{\partial\rho}{\partial t} = \{H_{11}, \rho_{11}\} + \{H_{22}, \rho_{22}\} + 2\{V, \alpha\} \tag{37}$$

Note that the terms involving $V\beta$ responsible for population transfer between states 1 and 2 cancel from the evolution equation. Equation 37 conserves the total population, given by the phase-space trace of ρ, as it should.

The equations of motion for $\mathbf{q}_j(t)$ and $\mathbf{p}_j(t)$ (j = 1, 2, ..., N) are derived by substituting eq 36 into eq 37. We have for the left-hand side of the resulting expression

$$\text{LHS} = -\frac{1}{N}\sum_{k=1}^{N}\left[\dot{\mathbf{q}}_k\cdot\frac{\partial g(\Gamma - \Gamma_k)}{\partial\mathbf{q}} + \dot{\mathbf{p}}_k\cdot\frac{\partial g(\Gamma - \Gamma_k)}{\partial\mathbf{p}}\right] \tag{38}$$

The right side of the equation becomes

$$\text{RHS} = \frac{1}{N}\sum_{k=1}^{N}\left[-\frac{\partial H_k}{\partial\mathbf{p}}\cdot\frac{\partial g(\Gamma - \Gamma_k)}{\partial\mathbf{q}} + \left(\frac{\partial H_k}{\partial\mathbf{q}} + 2\frac{\partial V(\Gamma_k)}{\partial\mathbf{q}}\alpha_k\right)\cdot\frac{\partial g(\Gamma - \Gamma_k)}{\partial\mathbf{p}}\right] \tag{39}$$

where

$$H_k = \sigma_k H_{11}(\Gamma_k) + (1 - \sigma_k)H_{22}(\Gamma_k) = \frac{\mathbf{p}_k^2}{2m} + \sigma_k U_1(\mathbf{q}_k) + (1 - \sigma_k)U_2(\mathbf{q}_k) \tag{40}$$

which defines the diagonal diabatic potentials $U_n(\mathbf{q})$ (n = 1, 2).

Equating the coefficients of the terms $\partial g(\Gamma - \Gamma_k)/\partial\mathbf{q}$ and $\partial g(\Gamma - \Gamma_k)/\partial\mathbf{p}$ of the LHS and RHS expressions yields the modified classical equations of motion for the trajectory ensemble

DOI: 10.1021/acs.jpca.8b10487
J. Phys. Chem. A 2019, 123, 1110−1128

$$\dot{\mathbf{q}}_j = \frac{\mathbf{p}_j}{m} \tag{41}$$

$$\dot{\mathbf{p}}_j = -\nabla U_j(\mathbf{q}_j) - 2\alpha_j \nabla V(\mathbf{q}_j) \tag{42}$$

for j = 1, 2, ..., N, where $\nabla \equiv \partial/\partial\mathbf{q}$. In addition to the classical force acting on the jth trajectory resulting from the instantaneous Hamiltonian, H_j, an additional quantum force appears, which depends on both the gradient of the off-diagonal diabatic coupling, $V(\mathbf{q}_j)$, and the real part of the coherence parameter, $\alpha_j(t)$, corresponding to that trajectory. The nonclassical force contributes whenever coupling and coherence are present. In CSH, these continuous quantum forces replace the sudden impulsive momentum rescaling of FSSH. Each trajectory does not conserve the classical energy, $H_j(t)$. Rather, the total energy expectation value, $E(t) = \mathrm{Tr}(\hat{H}\hat{\rho}(t))$, is conserved on average over the ensemble. We have discussed the energy budget of nonadiabatic dynamics in detail in a recent paper.[13] We will examine this point in more detail below in the description of the approximate QTSH method.

The expression LHS = RHS resulting from equating eqs 38 and 39 is a single equation for the 2f unknowns $\dot{\mathbf{q}}_j$ and $\dot{\mathbf{p}}_j$ (j = 1, 2, ..., N). One possible solution is given by our quantum trajectory equations of motion, eqs 41 and 42. Other solutions are also possible. This is related to the general ambiguity associated with trajectory representations of quantum-state evolution in any quantum trajectory approach. We have discussed this issue in other contexts in previous publications.[32−35]

We note that the quantum trajectory equations of motion, eqs 41 and 42, (as well as the corresponding adiabatic expressions described below) also appear in other non-surface-hopping trajectory-based approaches to nonadiabatic dynamics, such as in the Meyer−Miller classical analogue approach[36−38] and in the recent work of Tao.[39,40]

We emphasize that no momentum rescaling is performed in the CSH method when electronic transitions occur. In general, individual trajectories representing a quantum system have no requirement to separately conserve energy,[13,32,34] and they do not do so in this method. We believe that energy conservation of individual trajectories imposed by momentum rescaling is too classical from a physical perspective. The trajectories in a surface-hopping ensemble comprise a statistical representation of an underlying quantum density matrix and should not separately be overinterpreted as being "real". In particular, there is no reason why they should individually conserve energy. In quantum mechanics, it is the expectation value of the Hamiltonian (and its moments) that should be conserved by the time evolution. Whereas the adoption of momentum rescaling can lead to accurate results in some situations by imposing correct asymptotic properties by hand, as it were, it also leads to serious problems such as spuriously frustrated hops and corresponding forbidden processes that are allowed by exact quantum dynamics.

From a mathematical perspective, momentum rescaling is undesirable because it violates the phase-space locality of the underlying coupled semiclassical Liouville equations. This locality is readily apparent in eqs 16 and 17, which highlights the symmetrical appearance of the transition-inducing terms in the equations: Every element of population that is induced to leave surface 1 by the term $-2V(\Gamma)\beta(\Gamma)/\hbar$ appears on surface 2 as $+2V(\Gamma)\beta(\Gamma)/\hbar$ at the same point $\Gamma = (\mathbf{q},\mathbf{p})$ in phase space. Momentum rescaling to impose energy conservation induces a spurious shift of the probability in the phase space upon a transition that is unjustified by, and in conflict with, the mathematical form of the underlying semiclassical Liouville equation.

Adiabatic Representation. The CSH method can be implemented equally well in the adiabatic representation, where electronic-state coupling appears through off-diagonal terms in the kinetic energy.[16,41,42] We start with the quantum-mechanical Hamiltonian and density matrix in the adiabatic representation. These are given by

$$\hat{H} = \begin{pmatrix} \hat{H}_{++} & \hat{W} \\ \hat{W}^{\dagger} & \hat{H}_{--} \end{pmatrix} \tag{43}$$

and

$$\hat{\rho}(t) = \begin{pmatrix} \hat{\rho}_{++}(t) & \hat{\rho}_{+-}(t) \\ \hat{\rho}_{-+}(t) & \hat{\rho}_{--}(t) \end{pmatrix} \tag{44}$$

respectively. The adiabatic eigenstates $\{|+\rangle,|-\rangle\}$ are defined in terms of the diabatic basis $\{|1\rangle,|2\rangle\}$ as

$$|+\rangle = |1\rangle \cos(\phi/2) + |2\rangle \sin(\phi/2) \tag{45}$$

$$|-\rangle = -|1\rangle \sin(\phi/2) + |2\rangle \cos(\phi/2) \tag{46}$$

where the mixing angle $\phi(\mathbf{q})$ is given by

$$\tan\phi(\mathbf{q}) = \frac{2V(\mathbf{q})}{U_1(\mathbf{q}) - U_2(\mathbf{q})} \tag{47}$$

Here $U_1(\mathbf{q})$ and $U_2(\mathbf{q})$ are the diagonal diabatic-state potentials, and $V(\mathbf{q})$ is the off-diagonal diabatic coupling.

In terms of these states, the off-diagonal nonadiabatic couplings are

$$\hat{W} = \langle +|\hat{T}|-\rangle = \frac{i\hbar}{2m}\nabla\phi(\mathbf{q})\cdot\hat{\mathrm{p}} + \frac{\hbar^2}{4m}\nabla^2\phi(\mathbf{q}) \tag{48}$$

and

$$\hat{W}^{\dagger} = \langle -|\hat{T}|+\rangle = -\hat{W} \tag{49}$$

The nonadiabatic coupling vector matrix element, $\mathbf{d}(\mathbf{q})$, is defined as

$$\mathbf{d}(\mathbf{q}) \equiv \langle +|\nabla|-\rangle \tag{50}$$

This can be evaluated for the nonadiabatic states in terms of the diabatic states and position-dependent angle, $\phi(\mathbf{q})$, yielding the result

$$\mathbf{d}(\mathbf{q}) = -\frac{1}{2}\nabla\phi(\mathbf{q}) \tag{51}$$

In terms of this quantity, the off-diagonal element $\hat{W} = \langle +|\hat{H}|-\rangle$ can be written as

$$\hat{W} = -\frac{i\hbar}{2}\left(\mathbf{d}(\mathbf{q})\cdot\frac{\hat{\mathbf{p}}}{m} + \frac{\hat{\mathbf{p}}}{m}\cdot\mathbf{d}(\mathbf{q})\right) \tag{52}$$

with $\hat{W}^{\dagger} = \langle -|\hat{H}|+\rangle = -\hat{W}$. In the semiclassical limit employed below, this becomes

$$W(\Gamma) = -i\hbar\mathbf{d}(\mathbf{q})\cdot\frac{\mathbf{p}}{m} \tag{53}$$

with $W^*(\Gamma) = -W(\Gamma)$.

DOI: 10.1021/acs.jpca.8b10487
J. Phys. Chem. A 2019, 123, 1110−1128

By evaluating the Wigner transform of the quantum Liouville equation in the adiabatic representation, eq 12, to lowest order in $\hbar$, we obtain the corresponding semiclassical Liouville equations in the adiabatic representation[12,16,41]

$$\frac{\partial \rho_{++}}{\partial t} = \{H_{++}, \rho_{++}\} - \hbar\left\{\mathbf{d}\cdot\frac{\mathbf{p}}{m}, \beta\right\} - 2\mathbf{d}\cdot\frac{\mathbf{p}}{m}\alpha \tag{54}$$

$$\frac{\partial \rho_{--}}{\partial t} = \{H_{--}, \rho_{--}\} - \hbar\left\{\mathbf{d}\cdot\frac{\mathbf{p}}{m}, \beta\right\} + 2\mathbf{d}\cdot\frac{\mathbf{p}}{m}\alpha \tag{55}$$

$$\frac{\partial \alpha}{\partial t} = \{H_o, \alpha\} + \omega\beta + \mathbf{d}\cdot\frac{\mathbf{p}}{m}(\rho_{++} - \rho_{--}) \tag{56}$$

$$\frac{\partial \beta}{\partial t} = \{H_o, \beta\} - \omega\alpha - \frac{\hbar}{2}\left\{\mathbf{d}\cdot\frac{\mathbf{p}}{m}, \rho_{++} + \rho_{--}\right\} \tag{57}$$

where $H_{++}(\Gamma) = \mathbf{p}^2/2m + E_+(\mathbf{q})$, $H_{--}(\Gamma) = \mathbf{p}^2/2m + E_-(\mathbf{q})$, $H_o = \frac{1}{2}(H_{++} + H_{--})$, and $\omega(\Gamma) = (E_+(\mathbf{q}) - E_-(\mathbf{q}))/\hbar$; here $E_+(\mathbf{q})$ and $E_-(\mathbf{q})$ are the adiabatic potentials, the position-dependent eigenvalues of the diabatic potential matrix. The density matrix elements $\rho_{mn}(\Gamma,t)$ are now phase-space functions, and we have written the coherence $\rho_{+-} = \alpha + i\beta$ in terms of its real and imaginary parts.

The phase-space-generalized densities in the adiabatic representation are written in terms of an ensemble of N trajectories as

$$\rho_{++}(\Gamma, t) = \frac{1}{N}\sum_{j=1}^{N}\sigma_j(t)g(\Gamma - \Gamma_j(t)) \tag{58}$$

$$\rho_{--}(\Gamma, t) = \frac{1}{N}\sum_{j=1}^{N}(1 - \sigma_j(t))g(\Gamma - \Gamma_j(t)) \tag{59}$$

$$\alpha(\Gamma, t) = \frac{1}{N}\sum_{j=1}^{N}\alpha_j(t)g(\Gamma - \Gamma_j(t)) \tag{60}$$

$$\beta(\Gamma, t) = \frac{1}{N}\sum_{j=1}^{N}\beta_j(t)g(\Gamma - \Gamma_j(t)) \tag{61}$$

A similar analysis to the one performed above for the diabatic case then yields the CSH equations of motion for the quantum-state parameters and phase-space trajectories.

The stochastic parameters $\{\sigma_j\}$ (j = 1, 2, ..., N) are updated as follows. For the jth trajectory at phase-space point $\Gamma_j = (\mathbf{q}_j(t),\mathbf{p}_j(t))$ currently occupying state $|+\rangle$, the probability of hopping to state $|-\rangle$ at time t during a time interval Δt is given by

$$P_{\text{hop}}^{\text{CSH}} = \Delta\sigma_j = \left|\frac{2}{\langle\rho_{++}\rangle}\frac{\mathbf{d}(\mathbf{q}_j)\cdot\mathbf{p}_j}{m}\langle\alpha\rangle_j\Delta t\right| \tag{62}$$

with an analogous expression for hops from $|-\rangle \rightarrow |+\rangle$. The equations of motion for the coherence parameters yield the differential equations

$$\dot{\alpha}_j = \omega(\Gamma_j)\beta_j + \frac{\mathbf{d}(\mathbf{q}_j)\cdot\mathbf{p}_j}{m}(2\sigma_j - 1) \tag{63}$$

$$\dot{\beta}_j = -\omega(\Gamma_j)\alpha_j(t) \tag{64}$$

The trajectory equations of motion for $\mathbf{q}_j(t)$ and $\mathbf{p}_j(t)$ can be derived from the equation of motion for the total nuclear density $\rho = \rho_{++} + \rho_{--}$ using the same procedure employed above in the diabatic case. The result is

$$\dot{\mathbf{q}}_j = \frac{\mathbf{p}_j}{m} - 2\hbar\beta_j\frac{\mathbf{d}(\mathbf{q}_j)}{m} \tag{65}$$

$$\dot{\mathbf{p}}_j = -\nabla U_j(\mathbf{q}_j) + \frac{2\hbar}{m}\beta_j(\mathbf{p}_j\cdot\nabla)\mathbf{d}(\mathbf{q}_j) \tag{66}$$

for j = 1, 2, ..., N. The second term can also be written in terms of the time derivative of the nonadiabatic coupling vector along the resulting trajectories $\dot{\mathbf{d}} = (\mathbf{v}\cdot\nabla)\mathbf{d}$, where $\mathbf{v} = \mathbf{p}/m$ is the trajectory velocity

$$\dot{\mathbf{p}}_j = -\nabla U_j(\mathbf{q}_j) + 2\hbar\beta_j\dot{\mathbf{d}}(q_j) \tag{67}$$

In numerical implementation, it is much easier to determine the time derivative of $\mathbf{d}$ along a trajectory than to evaluate the spatial derivatives directly.

These equations of motion are closely related to those appearing in the Miller−Meyer treatment of coupled electronic-nuclear dynamics.[36−38] In ref 38, Miller and coworkers introduce a non-Hamiltonian "kinematic momentum", given in our notation by $\mathbf{p}_{\text{kin},j} = \mathbf{p}_j - 2\hbar\beta_j\mathbf{d}(\mathbf{q}_j)$, and show that its use simplifies numerical calculations by avoiding the appearance of $\nabla\mathbf{d}$. This approach may also be useful in the numerical application of the present method.

The quantum forces acting on the classical trajectories in the adiabatic representation are in the form of Hamilton's equations in the presence of a vector potential $\mathbf{A}(\mathbf{q},\beta(t))$

$$H(\Gamma, \sigma, \beta) = \frac{(\mathbf{p} - \mathbf{A}(\mathbf{q}, \beta(t)))^2}{2m} + U_\sigma(\mathbf{q}) \tag{68}$$

where $\mathbf{A}(\mathbf{q},\beta(t)) = 2\hbar\beta(t)\mathbf{d}(\mathbf{q})$ (neglecting terms of order $\hbar^2$). This vector potential depends on the quantum subsystem dynamics through the appearance of the imaginary part of the coherence, $\beta_j(t)$. Interesting geometric phase effects resulting from these nonclassical forces may result in systems with two or more dimensions in the presence of, for example, conical intersections.[43−47] This will be explored in future work.

The CSH method is based on a systematic derivation of the equations of motion for a trajectory ensemble representation of the nonadiabatic dynamics from the underlying quantum Liouville equation in the semiclassical limit. CSH eliminates the ad hoc instantaneous momentum rescaling and strict energy conservation of FSSH by incorporating continuous state-dependent quantum forces into the trajectory equations of motion. In addition, a correct treatment of quantum coherence emerges naturally in the CSH formalism through the collective and interdependent nature of the trajectories across the ensemble in determining hopping probabilities. The numerical implementation of the method can be quite accurate for model systems. However, the interdependent nature of the trajectories greatly increases the numerical cost of the method in direct implementations. For multidimensional systems, the CSH method quickly becomes prohibitively expensive with increasing size. Furthermore, the complexity of the method can lead to errors if conditions and parameters such as the Gaussian smoothing width are not chosen carefully. The main value of CSH is not as a practical method per se but as a framework for introducing further approximations in a well-controlled manner

DOI: 10.1021/acs.jpca.8b10487
J. Phys. Chem. A 2019, 123, 1110−1128

2.3. Quantum Trajectory Surface Hopping. We now describe a new surface-hopping approach based on an independent trajectory limit of the full CSH formalism. We provide a derivation of the individual trajectory quantum electronic-state density matrix dynamics and stochastic hopping algorithm for the independent trajectories of the FSSH method by employing additional well-defined approximations to CSH. The ad hoc impulsive momentum jumps of FSSH are abandoned, however, and replaced by the continuous quantum forces that emerge from the CSH formalism. We call the resulting method QTSH, a quantum trajectory-based variant of FSSH with a rigorous foundation.

In the CSH methodology, the underlying focus is on solving the coupled evolution of the phase-space functions $\rho_{mn}(\Gamma,t)$ using a trajectory ensemble representation. This naturally leads to the appearance of ensemble-level quantities in the equations of motion for the phase-space trajectories and quantum parameters. Consider, for example, the stochastic hopping of the jth trajectory from state 1 to state 2 in the diabatic representation. The local values of the functions representing state 1 population density $\rho_{11}(\Gamma,t) = (1/N)\sum_j \sigma_j(t) g(\Gamma - \Gamma_j(t))$ and the imaginary part of the coherence $\beta(\Gamma,t) = (1/N)\sum_j \beta_j(t) g(\Gamma - \Gamma_j(t))$ at the phase-space point $\Gamma = \Gamma_j$ determine the CSH hopping probability of trajectory j through the expression

$$P_{\text{hop}}^{\text{CSH}} = \left| \frac{1}{\langle \rho_{11} \rangle_j} \frac{2V(\Gamma_j)}{\hbar} \langle \beta \rangle_j \Delta t \right| \tag{69}$$

where $\langle \rho_{11} \rangle_j = \rho_{11}(\Gamma_j)$ and $\langle \beta \rangle_j = \beta(\Gamma_j)$.

This "consensus" involvement of the entire ensemble in the hopping decision making emerges systematically from first principles. The rigor of the methodology comes with a relatively high cost of numerical effort, however, as the local values of these quantities at every trajectory point Γ_j for (j = 1, 2, ..., N) must be determined from the ensemble as a whole at each time step. It is therefore desirable to introduce further well-controlled approximations to seek a "disentangling" of the ensemble to yield an approximate independent trajectory method, perhaps with ensemble-level corrections. One such approximate method, QTSH, will now be described.

The FSSH algorithm proposed by Tully relies on an assumption of consistency between two complementary representations of the quantum evolution—the trajectory populations of the electronic states and the corresponding individual trajectory auxiliary quantum density matrix populations.[1] We seek to establish a rigorous connection between Tully's ensemble of auxiliary density matrices and the local values of the CSH phase-space functions and its relation to surface-hopping consistency.

Returning to the hopping of the jth trajectory in our example, recall that the ensemble representation of the local phase-space population density at phase-space point $\Gamma = \Gamma_j$ on state 1 is

$$\langle \rho_{11} \rangle_j = \frac{1}{N} \sum_{k=1}^{N} \sigma_k g(\Gamma_j - \Gamma_k) \tag{70}$$

We now make the assumption that the stochastic variables, σ_k, have a well-defined local average $\langle \sigma \rangle_j$ in the phase-space region $|\Gamma_j - \Gamma_k| \leq \Delta\Gamma$, where $\Delta\Gamma$ is the width of the Gaussian function, $g(\Gamma)$. This suggests the approximation

$$\langle \rho_{11} \rangle_j \simeq \frac{1}{N} \sum_{k=1}^{N} \langle \sigma \rangle_j g(\Gamma_j - \Gamma_k) = \langle \sigma \rangle_j \langle \rho \rangle_j \tag{71}$$

where $\langle \rho \rangle_j$ is the local value of the total nuclear density $\rho = \rho_{11} + \rho_{22}$ at point Γ_j. Now consider the local value of the phase-space function representing the imaginary part of the coherence at Γ_j

$$\langle \beta \rangle_j = \frac{1}{N} \sum_{k=1}^{N} \beta_k g(\Gamma_j - \Gamma_k) \tag{72}$$

Here we make the simplifying assumption that the system is fully coherent, in the sense that the parameters β_k are slowly varying in the vicinity of Γ_j with values of the index k corresponding to $|\Gamma_j - \Gamma_k| \leq \Delta\Gamma$. For small enough $\Delta\Gamma$, we can then make the replacement $\beta_k \to \beta_j$ in the expression, giving the approximation

$$\langle \beta \rangle_j \simeq \frac{1}{N} \sum_{k=1}^{N} \beta_j g(\Gamma_j - \Gamma_k) = \beta_j \langle \rho \rangle_j \tag{73}$$

Under these approximations, the CSH hopping probability becomes

$$P_{\text{hop}}^{\text{CSH}}(t) \simeq \left| \frac{1}{\langle \sigma \rangle_j \langle \rho \rangle_j} \frac{2V(\Gamma_j)}{\hbar} \beta_j \langle \rho \rangle_j \Delta t \right| = \left| \frac{1}{\langle \sigma \rangle_j} \frac{2V(\Gamma_j)}{\hbar} \beta_j \Delta t \right| \tag{74}$$

with the total nuclear density at point Γ_j canceling from numerator and denominator.

The connection between the independent limit of CSH and the conventional FSSH formalism can now be made. Within the consistency assumption underlying FSSH, the populations of the auxiliary density matrix elements of each trajectory should agree with the state population statistics of the trajectory ensemble. We assume that the proper correspondence should hold locally in the phase space, so the independent trajectory population $a_{11,j}(t)$ should be equated with the appropriate local average behavior of the ensemble. In our notation

$$a_{11,j}(t) = \langle \sigma \rangle_j(t) \tag{75}$$

With these identifications, we finally arrive at the QTSH hopping probability expression

$$P_{\text{hop}}^{\text{QTSH}}(t) = \left| \frac{1}{a_{11,j}} \frac{2V(\Gamma_j)}{\hbar} \beta_j \Delta t \right| \tag{76}$$

which is identical to the corresponding FSSH result, eq 11. The consistency assumption of FSSH further assumes that the $a_{kl}(t)$ parameters can be computed by solving the auxiliary quantum equations of motion for each trajectory, eq 6.

A similar line of reasoning gives the QTSH hopping probability in the adiabatic representation

$$P_{\text{hop}}^{\text{QTSH}} = \left| \frac{2}{a_{++,j}} \frac{\mathbf{d}(\mathbf{q}_j)\cdot \mathrm{p}_j}{m} \alpha_j \Delta t \right| \tag{77}$$

In this independent trajectory limit, $\langle \rho_{++} \rangle_j \to a_{++,j} \langle \rho \rangle_j$ and $\langle \alpha \rangle_j \to \alpha_j \langle \rho \rangle_j$

DOI: 10.1021/acs.jpca.8b10487
J. Phys. Chem. A 2019, 123, 1110−1128

The numerical implementation of the QTSH method uses the following procedure (given here for the adiabatic representation): The continuous equations, eq 6, for the quantum subsystem of each trajectory are integrated to determine the smoothly varying quantities $a_{++,j}$, $a_{--,j}$, α_j, and β_j. In addition, the stochastic variable σ_j is propagated using the probabilistic algorithm in eq 77. The classical variables are propagated under the influence of the instantaneous Hamiltonian $H_j = \sigma_j H_{++} + (1 - \sigma_j)H_{--}$ augmented by the CSH nonclassical terms derived above, eqs 65 and 66. The classical forces in the equations of motion change discontinuously at the points of transition, whereas the nonclassical forces are continuous there. The resulting phase-space path $(\mathbf{q}_j(t),\mathbf{p}_j(t))$ is continuous, unlike in the FSSH method, as we do not rescale the momenta to impose energy conservation.

Energy Conservation. The FSSH method for surface hopping imposes strict conservation of the classical energy of each independent trajectory $H_j(\Gamma_j(t),t) = E_j$, where in our notation $H_j(\Gamma,t) = \sigma_j(t)H_1(\Gamma) + (1 - \sigma_j(t))H_2(\Gamma)$ and E_j is the initial classical energy. This is accomplished by the ad hoc rescaling of the individual trajectory momenta at the time of each hop, which imposes energy conservation on each trajectory by hand.

Quantum mechanics, of course, requires energy conservation as well but at the state level. Furthermore, the full Hamiltonian $\hat{H}$ and density matrix $\hat{\rho}$ are involved, not just the diagonal elements. The total conserved energy of the quantum system is the operator trace $E = \mathrm{Tr}(\hat{H}\hat{\rho})$, and its quantum-classical limit is given by the corresponding classical trace

$$E(t) = \mathrm{Tr}H\rho = \int \mathbf{H}(\Gamma)\rho(\Gamma, t)\, \mathrm{d}\Gamma \tag{78}$$

where the integral is over the $2f$-dimensional phase space. Here both $\mathbf{H}(\Gamma)$ and $\boldsymbol{\rho}(\Gamma,t)$ are 2×2 matrices of the corresponding classical-limit phase-space functions. Writing this out in terms of the matrix elements in the diabatic representation gives

$$\begin{aligned} E(t) &= \mathrm{Tr}(H\rho) \\ &= \mathrm{Tr}(H_{11}\rho_{11}) + \mathrm{Tr}(H_{22}\rho_{22}) + 2\mathrm{ReTr}(V\rho_{12}) \end{aligned} \tag{79}$$

or

$$E(t) = \mathrm{Tr}(H_{11}\rho_{11}) + \mathrm{Tr}(H_{22}\rho_{22}) + 2\mathrm{Tr}(V\alpha) \tag{80}$$

The total energy consists of three terms

$$E = E_1 + E_2 + E_{\mathrm{coh}}^{\mathrm{dia}} \tag{81}$$

In terms of the trajectory representation, this becomes

$$E = \frac{1}{N}\sum_{j=1}^{N} \sigma_j H_{11}(\Gamma_j) + (1 - \sigma_j)H_{22}(\Gamma_j) + 2V(\Gamma_j)\alpha_j \tag{82}$$

which defines the terms

$$E_1 = \frac{1}{N}\sum_{j=1}^{N} \sigma_j H_{11}(\Gamma_j) \tag{83}$$

$$E_2 = \frac{1}{N}\sum_{j=1}^{N} (1 - \sigma_j)H_{22}(\Gamma_j) \tag{84}$$

and

$$E_{\mathrm{coh}}^{\mathrm{dia}} = \frac{2}{N}\sum_{j=1}^{N} V(\Gamma_j)\alpha_j \tag{85}$$

The diagonal energy is the sum $E_{\mathrm{diag}} = E_1 + E_2$. It should be noted that the total energy, E, is *not* equal to E_{diag}. This diagonal energy is the quantity that FSSH rigorously conserves at the individual trajectory level by momentum rescaling. When coherence $\alpha_j \neq 0$ and the coupling $V(\Gamma_j)$ is present, a third *coherence energy* term, $E_{\mathrm{coh}}^{\mathrm{dia}}$, is required to balance the energy budget.[13]

We can write the total energy as the sum over single trajectory contributions

$$E(t) = \frac{1}{N}\sum_{j=1}^{N} E_j(t) \tag{86}$$

The QTSH method conserves this energy on average at the level of the consistency of the FSSH approach. To prove this, we take the time derivative of eq 82. This gives

$$\dot{E}(t) = \frac{1}{N}\sum_{j=1}^{N} \dot{E}_j(t) \tag{87}$$

where

$$\begin{aligned} \dot{E}_j(t) = \dot{\mathbf{p}}_j\cdot\frac{\mathbf{p}_j}{m} &+ \dot{\sigma}_j[U_1(\mathbf{q}_j) - U_2(\mathbf{q}_j)] \\ &+ \dot{\mathbf{q}}_j\cdot[\sigma_j\nabla U_1(\mathbf{q}_j) + (1 - \sigma_j)\nabla U_2(\mathbf{q}_j) \\ &+ 2\nabla V(\mathbf{q}_j)\alpha_j] + 2V(\mathbf{q}_j)\dot{\alpha}_j \end{aligned} \tag{88}$$

From the equations of motion for the density matrix elements, we have

$$\dot{\sigma}_j \simeq \dot{a}_{11,j} = -\frac{2V(\mathbf{q}_j)}{\hbar}\beta_j \tag{89}$$

$$\dot{\alpha}_j = \omega(\mathbf{q}_j)\beta_j = \frac{1}{\hbar}[U_1(\mathbf{q}_j) - U_2(\mathbf{q}_j)]\beta_j \tag{90}$$

where we have used $\omega = (H_{11} - H_{22})/\hbar$ and have indicated that the first equation holds on average.

For the phase-space variables $(\mathbf{q}_j,\mathbf{p}_j)$, we have the quantum trajectory equation of motion

$$\dot{\mathbf{q}}_j = \frac{\mathbf{p}_j}{m} \tag{91}$$

$$\dot{\mathbf{p}}_j = -[\sigma_j\nabla U_1(\mathbf{q}_j) + (1 - \sigma_j)\nabla U_2(\mathbf{q}_j)] - 2\nabla V(\mathbf{q}_j)\alpha_j \tag{92}$$

By eliminating $\dot{\mathbf{q}}_j$, $\dot{\mathbf{p}}_j$, $\dot{\sigma}_j$, and $\dot{\alpha}_j$ from the equation for $\dot{E}_j$, we can show the time derivative of each term vanishes on average, $\dot{E}_j \simeq 0$, so that

$$\dot{E}(t) = 0 \tag{93}$$

It should be noted that this energy conservation, which holds rigorously if $\sigma_j(t)$ evolves continuously, is not strictly obeyed at the individual trajectory level when a stochastic algorithm is employed to propagate σ_j. A sudden "hop" of $\sigma_j(t) = 0$ to $\sigma_j(t) = 1$, for instance, leads to an instantaneous change in the Hamiltonian $H_j = \sigma_j H_{11} + (1 - \sigma_j)H_{22}$ from H_{11} to H_{22}. However, on average, σ_j obeys the smooth differential equation, and so averaged over the ensemble the energy

DOI: 10.1021/acs.jpca.8b10487
J. Phys. Chem. A 2019, 123, 1110−1128

conservation of the state re-emerges. The assumptions required for this quantum energy conservation are equivalent to the consistency assumption underlying the surface-hopping method itself.

The same approach can be followed to show the average energy conservation in the adiabatic representation by using the adiabatic ensemble energy

$$E = \frac{1}{N}\sum_{j=1}^{N} \sigma_j H_{++}(\Gamma_j) + (1-\sigma_j)H_{--}(\Gamma_j) - 2\hbar \mathbf{d}(\mathbf{q}_j)\cdot\mathbf{p}_j\beta_j \tag{94}$$

and the corresponding adiabatic equations of motion for σ_j, α_j, β_j, $\mathbf{q}_j$, and $\mathbf{p}_j$. The diagonal and coherence contributions to the total energy, E, are then

$$E^{\text{adia}}_{\text{diag}} = \frac{1}{N}\sum_{j=1}^{N} \sigma_j H_{++}(\Gamma_j) + (1-\sigma_j)H_{--}(\Gamma_j) \tag{95}$$

and

$$E^{\text{adia}}_{\text{coh}} = -\frac{2\hbar}{N}\sum_{j=1}^{N} \mathbf{d}(\mathbf{q}_j)\cdot\mathbf{p}_j\beta_j \tag{96}$$

respectively. The equations of motion then lead to $\dot{E} = 0$ for the ensemble within the consistency assumption.

Conventional FSSH surface hopping imposes energy conservation by an accompanying rescaling of the momentum $\mathbf{p}_j \rightarrow \mathbf{p}_j + \Delta\mathbf{p}_j$. We stress here that this is not necessary and, in fact, is incorrect. The nonclassical term in the equations of motion for $(\mathbf{q}_j,\mathbf{p}_j)$ smoothly modifies the evolution of individual trajectories in the phase space and guarantee the average conservation of the state energy. This is the only rigorous energetic requirement of quantum dynamics.

Time Reversibility. Individual surface-hopping trajectories are not time-reversible due to the stochastic nature of their evolution. The time reversibility of the FSSH method is further sabotaged by two additional features of the method. First, the presence of frustrated hops breaks the consistency between the auxiliary quantum density matrices of individual trajectories and the population statistics of the ensemble in a manner that erodes the consistency of these quantities in a time-irreversible manner. Second, the energy-conserving momentum jumps introduce discontinuities in the classical phase-space evolution that cannot be back-integrated, even on average. The consequence of these features is that an ensemble of FSSH trajectories cannot be time-reversed. The lack of time reversibility of the state evolution represented by a time-dependent FSSH ensemble has led to much attention and effort being expended on exploring important but less rigorous requirements such as detailed balance.[48−50]

Unlike standard FSSH, the QTSH approach is manifestly time-reversible on average, within the consistency assumption. Individual trajectories are stochastic and thus lose strict time-reversal symmetry. These objects, however, are not "knowable" parts of a quantum theoretical description. Quantum mechanics describes the evolution of states that in a trajectory context places constraints only on ensemble behavior with nothing to say about its individual members. The QTSH approach formally satisfies time reversibility: An initial density matrix $\rho_o(\Gamma,0)$ propagated for a given system from $t = 0$ to $t = T$ will produce an intermediate state $\rho_{\text{int}}(\Gamma,T)$. The reversal of the signs of all intermediate momenta and imaginary parts of the auxiliary density matrices $\mathbf{p}_j(T) \rightarrow -\mathbf{p}_j(T)$ and $\beta_j(T) \rightarrow -\beta_j(T)$ ($j = 1, 2, ..., N$) produces another ensemble. Propagation for an additional time period, T, then is equivalent to integrating the system dynamics back to $t = 0$. Formally, this will reproduce a final state $\rho_f(\Gamma,2T)$ that is equivalent to the initial ensemble, $\rho_o(\Gamma,0) = \rho_f(\Gamma,2T)$, although differing in the details of each trajectory's dynamical variables. This is confirmed in numerical simulations, as we will see below.

Decoherence Corrections. The QTSH method is an independent trajectory limit of the CSH formalism. This reintroduces the problem of "overcoherence" that characterizes the standard FSSH approach. In our notation, this corresponds to approximating the ensemble-level representation of the coherence by the individual trajectory contributions, for example: $\langle\alpha\rangle_j \simeq \alpha_j\langle\rho\rangle$. In some situations, this is an accurate approximation, but in cases where pure-state dynamics or system-bath interactions lead to significant variation of the phase of trajectories over the local neighborhoods of trajectories, this approximation will lead to an overestimation of the hopping probabilities. Many attempts have been made to develop decoherence corrections in the context of the FSSH approach (see, e.g., refs 9 and 10).

Here we propose a simple empirical ensemble-level decoherence correction. Rather than employing a theoretical approach based on approximations to the underlying equations of motion, we estimate the quantities $\langle\alpha\rangle_j$ and $\langle\beta\rangle_j$ empirically from the statistics of the evolving trajectory ensemble itself.

We define a proxy phase for each trajectory, ϕ_j ($j = 1, 2, ..., N$), given by

$$\phi_j(t) = \int_0^t \omega(\mathbf{q}_j(t'))\,\mathrm{d}t' \tag{97}$$

This quantity is not identical to the phase of the complex number $\alpha_j(t) + i\beta_j(t)$ that represents the coherence of the jth trajectory, which may be undefined or have a particular nonzero value at $t = 0$, but rather is a phase-like quantity for that trajectory that can be compared across the ensemble. To do so, we calculate the ensemble averages of the phase and its square

$$\langle\phi(t)\rangle = \frac{1}{N}\sum_{j=1}^{N}\phi_j(t) \tag{98}$$

$$\langle\phi^2(t)\rangle = \frac{1}{N}\sum_{j=1}^{N}\phi_j^2(t) \tag{99}$$

which then allows the time-dependent phase variance $\delta\phi^2(t)$ over the ensemble to be defined

$$\delta\phi^2(t) = \langle\phi^2(t)\rangle - \langle\phi(t)\rangle^2 \tag{100}$$

By assuming Gaussian statistics, we can define a global time-dependent decoherence factor $\chi(t)$

$$\chi(t) = \mathrm{e}^{-1/2\delta^2\phi(t)} \tag{101}$$

Unlike most other approaches, which estimate decoherence corrections to independent trajectory coherences from local properties, we determine $\chi(t)$ from the nonlocal characteristics of the ensemble as a whole, in line with the lessons learned from the full CSH formalism.

A decoherence-corrected version of QTSH can then be implemented by incorporating the correction factor, χ, into the hopping probabilities of the individual trajectories.

DOI: 10.1021/acs.jpca.8b10487
J. Phys. Chem. A 2019, 123, 1110−1128

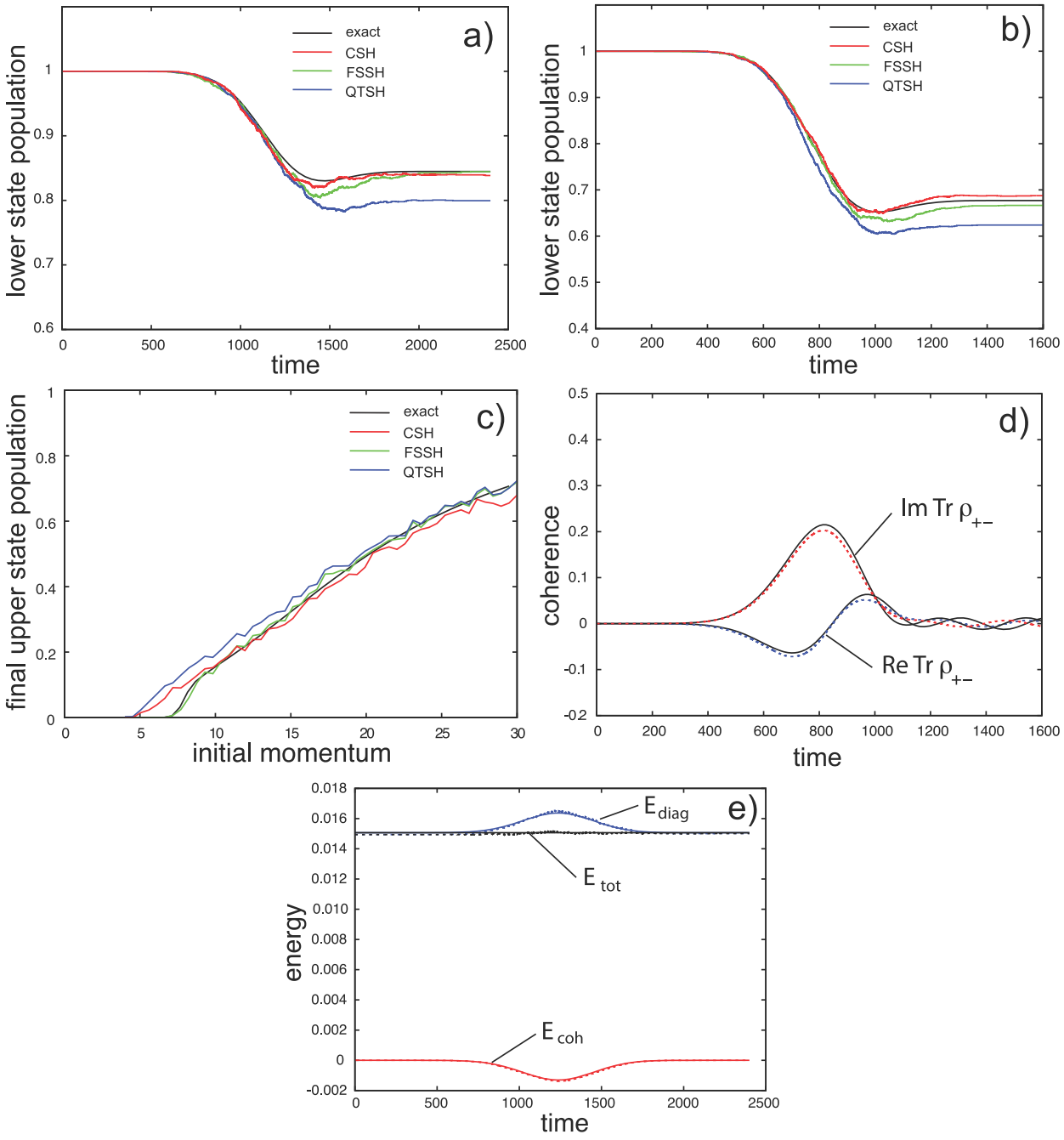

Figure 1. (a,b) Time dependence of the lower adiabatic state population for Tully's single-crossing model. The FSSH (green), QTSH (blue), and CSH (red) results are compared with exact wavepacket calculations (black). (a) $\hbar k = 10$. (b) $\hbar k = 15$. (c) Final upper state population is shown as a function of the initial momentum $\hbar k$. (d) Coherence for $\hbar k = 15$. Exact (black solid) and QTSH (dashed) results for the real (blue) and imaginary (red) parts of $\mathrm{Tr}\rho_{12}$ are compared. See the text for details. (e) Energy budget for the $\hbar k = 10$ state is shown. Exact quantum results (black solid) are compared with the QTSH ensemble (dashed colored). See the text for discussion. Calculations are done in the adiabatic representation.

$$P_{\mathrm{hop}}^{\mathrm{QTSH}}(t) \rightarrow \left| \frac{2}{a_{++,j}} d(q_j) \frac{p_j}{m} (\chi \alpha_j) \Delta t \right| \tag{102}$$

This modified hopping algorithm makes the egalitarian approximation $\langle \alpha \rangle_j \simeq \chi \alpha_j \langle \rho \rangle$ for $j = 1, 2, ..., N$. It should be noted that this approach retains the full coherence of the individual trajectories during their propagation but modifies the probability of hopping during each time step using the global-ensemble-level decoherence factor, $\chi(t)$. Most other approaches add dissipation to the equations of motion for the terms $\alpha_j(t)$ themselves, introducing a pure dephasing component to the quantum evolution that leads to a mixed-state density matrix even for pure-state dynamics. The

DOI: 10.1021/acs.jpca.8b10487
J. Phys. Chem. A 2019, 123, 1110−1128

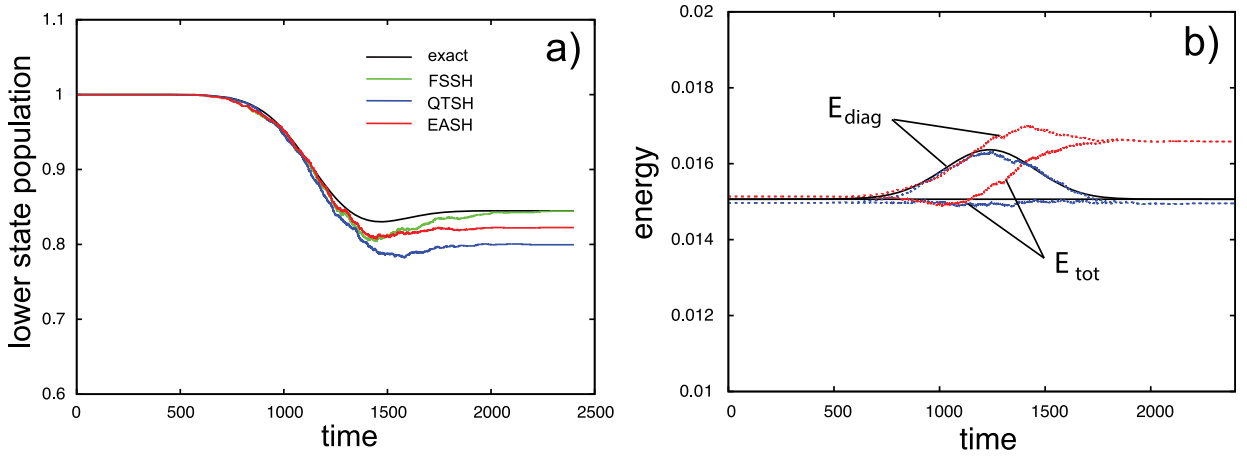

Figure 2. Comparison of FSSH and QTSH with an "energy aloof" variant, EASH. (a) Time dependence of the adiabatic lower state population for Tully's single-crossing model with $\hbar k = 10$. The FSSH (green), QTSH (blue), and EASH (red) results are compared with exact wavepacket calculations (black). (b) Energy budget for the state is shown. Exact quantum results (black solid) are compared with the QTSH (blue) and EASH (red). The total, E_{tot}, and diagonal, E_{diag}, contributions are shown as a function of time. See the text for discussion.

approach here is derived from the full CSH formalism as a well-defined approximation and, we feel, is more faithful to the underlying exact quantum evolution.

The ensemble-level correction described here is based on the simplest possible assumption regarding the relationship between the evolving phase-space function $\rho_{12}(\Gamma,t)$ (or $\rho_{+-}(\Gamma,t)$ in the adiabatic representation) and its representation as an ensemble of trajectories: The local interplay of the phases of individual trajectories can be represented uniformly across the ensemble by a single average factor, χ. More elaborate and complicated methods can be imagined, where variations of the effect are estimated theoretically or statistically. The advantage of the current proposal is its simplicity and numerical efficiency. In particular, if the system under study is simple enough that the entire ensemble of trajectories can be propagated in parallel, then the averages required to estimate χ lead to a negligible additional cost to the calculations. Large systems where the trajectories comprising the ensemble must be integrated independently will require a different approach. In the next section, we will test this simple decoherence correction.

3. RESULTS

In this section, we briefly illustrate the numerical implementation of the QTSH method and compare it with exact quantum-wavepacket results and standard FSSH for several simple systems. We highlight both the strengths and shortcomings of the QTSH approach. More thorough numerical benchmarking of CSH, QTSH, and decoherence corrections will be given in a future publication.

We apply the QTSH method to two model systems originally proposed by Tully as benchmark problems and adopted universally by the surface-hopping community as test cases.[1] The first is Tully's single-crossing system, which is a 1D model corresponding to two electronic surfaces undergoing a single crossing. The system has been treated in many previous publications. We adopt the potentials and parameters from Tully's original paper[1] and treat ensembles of 2000 trajectories sampled randomly from an initial minimum uncertainty phase-space Gaussian distribution with spatial width $\sigma_q = 1.0$ and with mean initial position $q_o = -6$. A range of ensembles with varying initial mean momenta $p_o = \hbar k$ is generated and propagated using the QTSH method. The results are compared with standard FSSH and corresponding quantum-wavepacket calculations using the method of Kosloff.[51]

In Figure 1, we show results obtained for Tully's single-crossing system.[1] Here calculations are performed in the adiabatic representation for the QTSH method and compared with standard FSSH[1] as well as the full CSH approach[12] (incorporating the modified classical equations of motion described above) and quantum-wavepacket calculations. In Figure 1a,b, we show the time dependence of the population of the initially occupied lower adiabatic state as a function of time for initial momenta $\hbar k = 10$ and $\hbar k = 15$, respectively. In Figure 1c, the dependence of the final population of the upper adiabatic state on the initial momentum $\hbar k$ is given.

All of the methods are in reasonable agreement with the exact quantum results. For this system, the FSSH method gives superior agreement for low momenta ($k < 8$), presumably due to the explicit imposition of energy conservation; here the presence of frustrated hops improves the results. For higher energies, the CSH method gives slightly better agreement with the quantum results. For this system, the QTSH method slightly overestimates the extent of nonadiabatic transition. The asymptotic energetic constraints imposed by FSSH must emerge naturally here from the method itself, and the independent trajectory approximation apparently leads to overcoherence and thus too extensive population transfer that is corrected for by the FSSH energy constraint. We will return to this point below in the context of the ensemble-level decoherence correction.

In Figure 1d, we investigate the agreement between exact quantum and QTSH ensemble dynamics in more detail. For the state with an initial momentum of $\hbar k = 15$ we show a comparison of exact and QTSH values for $\mathrm{Tr}\,\rho_{12}$, a metric for the total coherence of the evolving states. The exact quantum values were calculated by taking the time-dependent overlap of the adiabatic-state wavepackets. The QTSH values for the real and imaginary parts are given by the ensemble averages of α_j and β_j, respectively. For this case, nearly quantitative agreement is observed, indicating that the evolving ensemble

DOI: 10.1021/acs.jpca.8b10487
J. Phys. Chem. A 2019, 123, 1110−1128

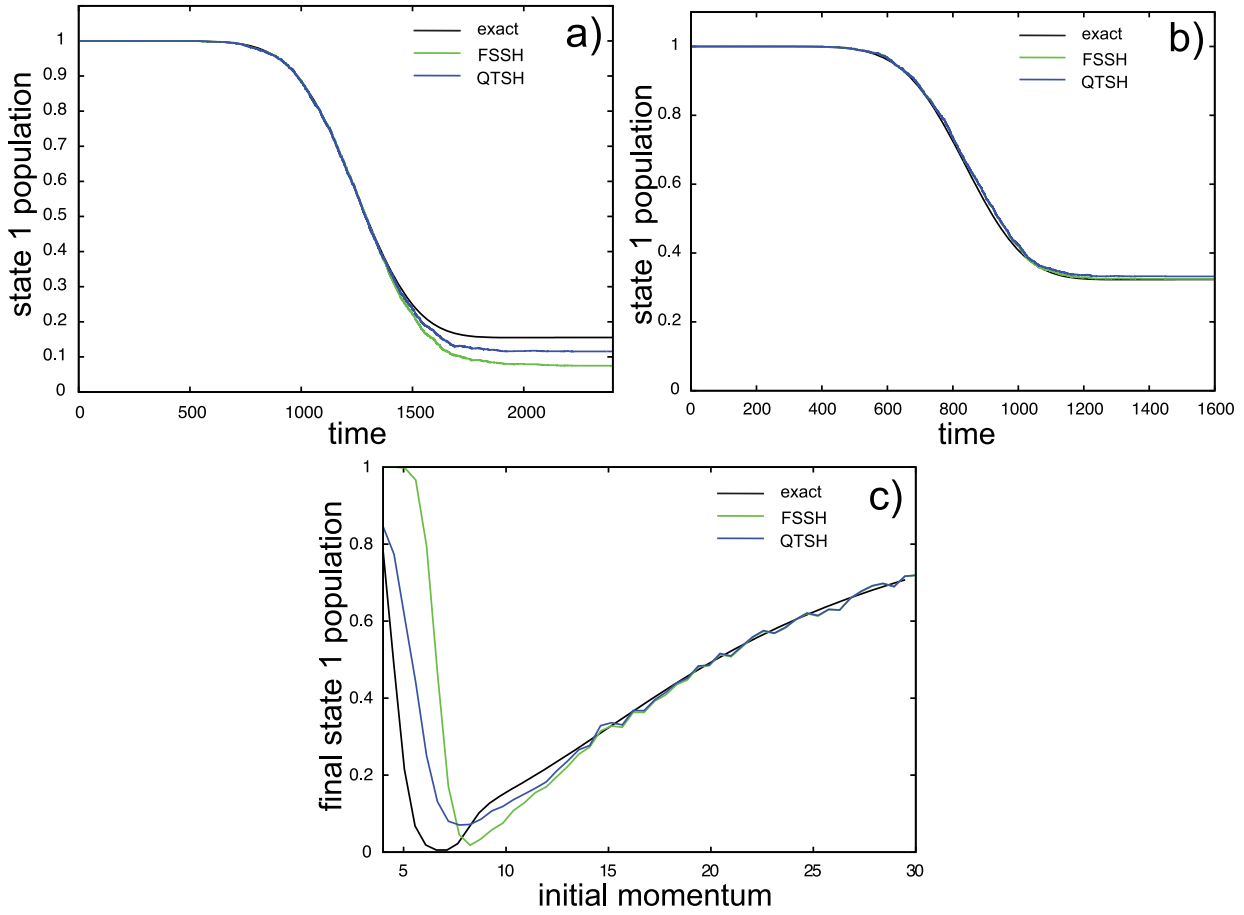

Figure 3. (a,b) Time dependence of the diabatic state 1 population for Tully's single-crossing model. The FSSH (green) and QTSH (blue) results are compared with exact wavepacket calculations (black). (a) $\hbar k = 10$. (b) $\hbar k = 15$. (c) Final state 1 population versus initial momentum $\hbar k$ is shown. Calculations are done in the diabatic representation.

of hopping trajectories is capturing well this feature of the fully coherent quantum dynamics.

Despite the error in population transfer, the QTSH method correctly conserves the quantum-classical energy $E = \mathrm{Tr}(H\rho)$. In Figure 1d, we show the energy budget of the $\hbar k = 10$ ensemble by separately plotting the diagonal and coherence contributions to the total energy, given for the adiabatic representation by eqs 95 and 96, as well as their sum E_{tot}, and compare with a similar partitioning of the exact quantum energy. The QTSH total energy is constant and in agreement with the exact value to within numerical error. The classical diagonal energy is not constant, in contrast with the assumption of the FSSH formalism, but is compensated by the contribution of the coherence energy. The QTSH estimates of these are in essentially quantitative agreement with the quantum-mechanical results.

It is instructive to consider an even simpler surface-hopping simulation using a pared-down methodology defined by ignoring the energy conservation requirement and momentum rescaling of FSSH, or equivalently, by removing the nonclassical forces from QTSH. We compare this "energy aloof surface-hopping" variant, which we denote EASH, with FSSH and QTSH in Figure 2 for the Tully 1 $\hbar k = 10$ case in the adiabatic representation, considered in Figure 1. In Figure 2a, we show the time-dependent lower state population, whereas Figure 2b displays the energy budget of total and diagonal (e.g., classical) contributions. Removing the imposition of energy conservation leads to an overestimate of the nonadiabatic probability by EASH, as otherwise frustrated hops are allowed to occur. The results are not as accurate as FSSH but are still closer to the exact results than QTSH. A bigger difference is seen in Figure 2b), where the energetics of the evolution are displayed. QTSH (blue dashed lines) shows nearly quantitative agreement with the exact quantum diagonal and total energies (solid black lines). Neglecting the nonclassical forces of QTSH yields the EASH method (red dashed lines). The breakdown of energy conservation of EASH is clearly visible. Both the diagonal and total energies deviate from the exact values, and asymptotically the system has violated energy conservation by a nontrivial amount. For the FSSH method, the final total energy would be constrained to be conserved by the individual trajectory momentum rescaling, which conserved the diagonal (classical) contribution at all times.

This example illustrates the important point that the rigorous energy conservation of the QTSH method without momentum jumps is independent of the accuracy of the method. For this particular initial state, the EASH results are actually more accurate than QTSH, despite its failure to conserve energy.

DOI: 10.1021/acs.jpca.8b10487
J. Phys. Chem. A 2019, 123, 1110−1128

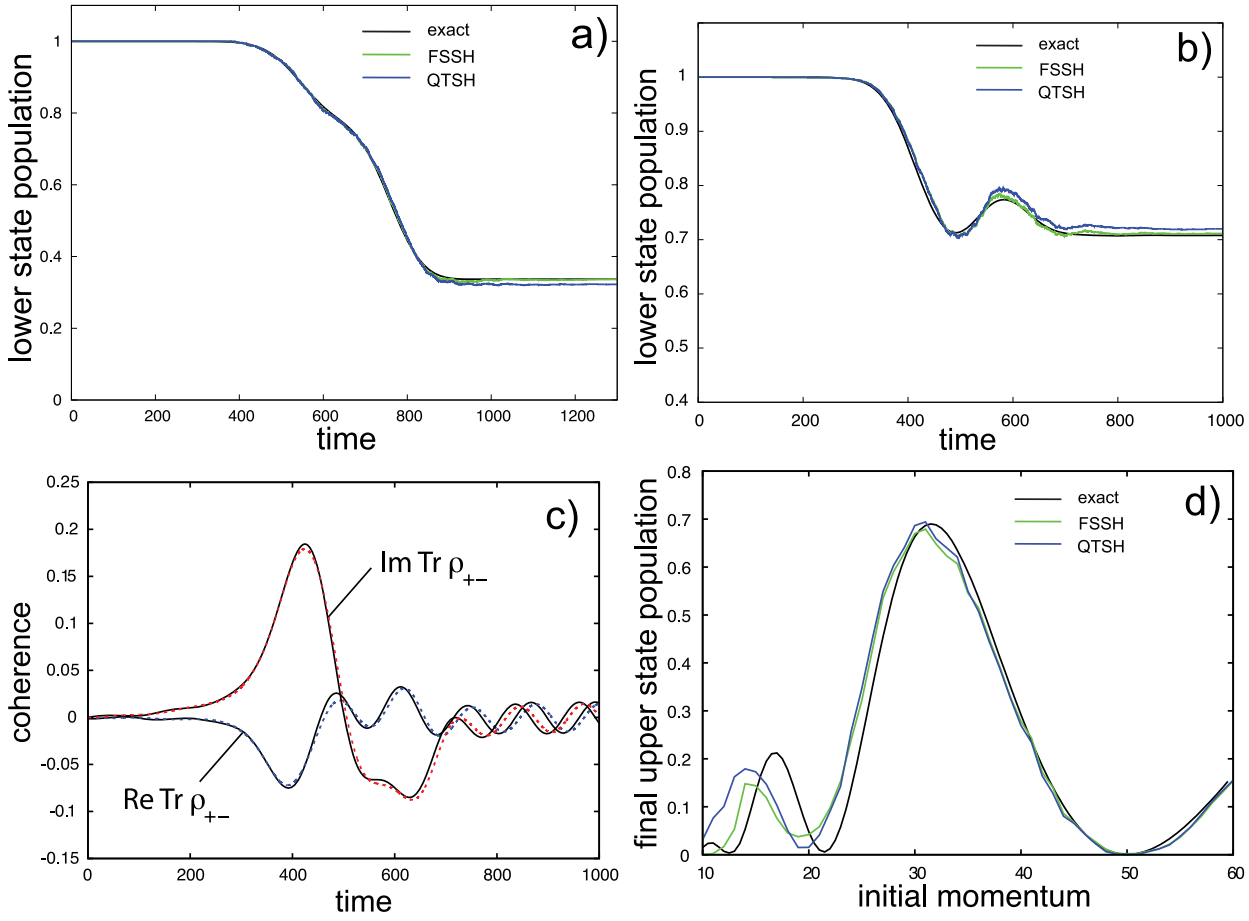

Figure 4. (a,b) Time dependence of the adiabatic lower state population for Tully's dual-crossing model. The FSSH (green) and QTSH (blue) results are compared with exact wavepacket calculations (black). (a) $\hbar k$ = 30. (b) $\hbar k$ = 40. (c) Coherence for $\hbar k$ = 40. Exact (black solid) and QTSH (dashed) results for the real (blue) and imaginary (red) parts of Trρ_{+-} are compared. See the text for details. (d) Final upper state population versus initial momentum $\hbar k$ is shown. Calculations are done in the adiabatic representation.

In Figure 3, we present results for the same initial states as presented in Figure 1 but calculated in the diabatic representation. The QTSH results are compared with FSSH and exact quantum-wavepacket calculations.

In Figure 3a,b, we show the time dependence of the population of the initially occupied diabatic state 1 as a function of time for initial momentum $\hbar k$ = 10 and $\hbar k$ = 15, respectively. In Figure 3c, the dependence of the final population of state 1 on the initial momentum $\hbar k$ is given. Again, close agreement between the methods is observed, with the QTSH results being in better agreement at lower k values in this case.

It should be emphasized that unlike FSSH the applicability of the QTSH formalism is independent of the electronic-state representation. For this 1D problem, the application of the FSSH in the diabatic representation is unambiguous, but in higher dimensions, the absence of the nonadiabatic coupling vector, **d**, in the diabatic formulation complicates the momentum rescaling component of the FSSH method. QTSH, on the contrary, can be straightforwardly and unambiguously applied in the diabatic representation.

In Figure 4, we consider Tully's dual-crossing model.[1] Results obtained using the QTSH method in the adiabatic representation are compared with FSSH and exact quantum-wavepacket calculations.

In Figure 4a,b, the populations of the initially occupied lower adiabatic state as a function of time for initial momenta $\hbar k$ = 30 and $\hbar k$ = 40 are shown, respectively. Figure 4c compares the real and imaginary parts of the QTSH coherence Trρ_{+-} for $\hbar k$ = 40. In Figure 4d, the dependence of the final population of the upper adiabatic state on the initial momentum $\hbar k$ is given. Again, close agreement is obtained except at low k, where both surface-hopping methods are slightly shifted from the exact quantum results.

Figure 5 presents results obtained by applying the QTSH method to the 1D three-state superexchange model introduced by Prezhdo and coworkers.[9,52] In this system, population transfer from the lowest-lying state 1 to final state 3 is calculated. These states are not directly coupled in the diabatic representation but are each coupled to a high-lying and, for some initial momenta, classically forbidden state 2. The system consists of three constant diagonal diabatic potentials coupled at the coordinate origin by off-diagonal potential couplings. The potential functions and system parameters are given in the original references.[9,52] We start an initial minimum uncertainty phase-space distribution with coordinate width σ_q = 1 and mean momentum $\hbar k$ to the left of the coupling region and use

DOI: 10.1021/acs.jpca.8b10487
J. Phys. Chem. A 2019, 123, 1110−1128

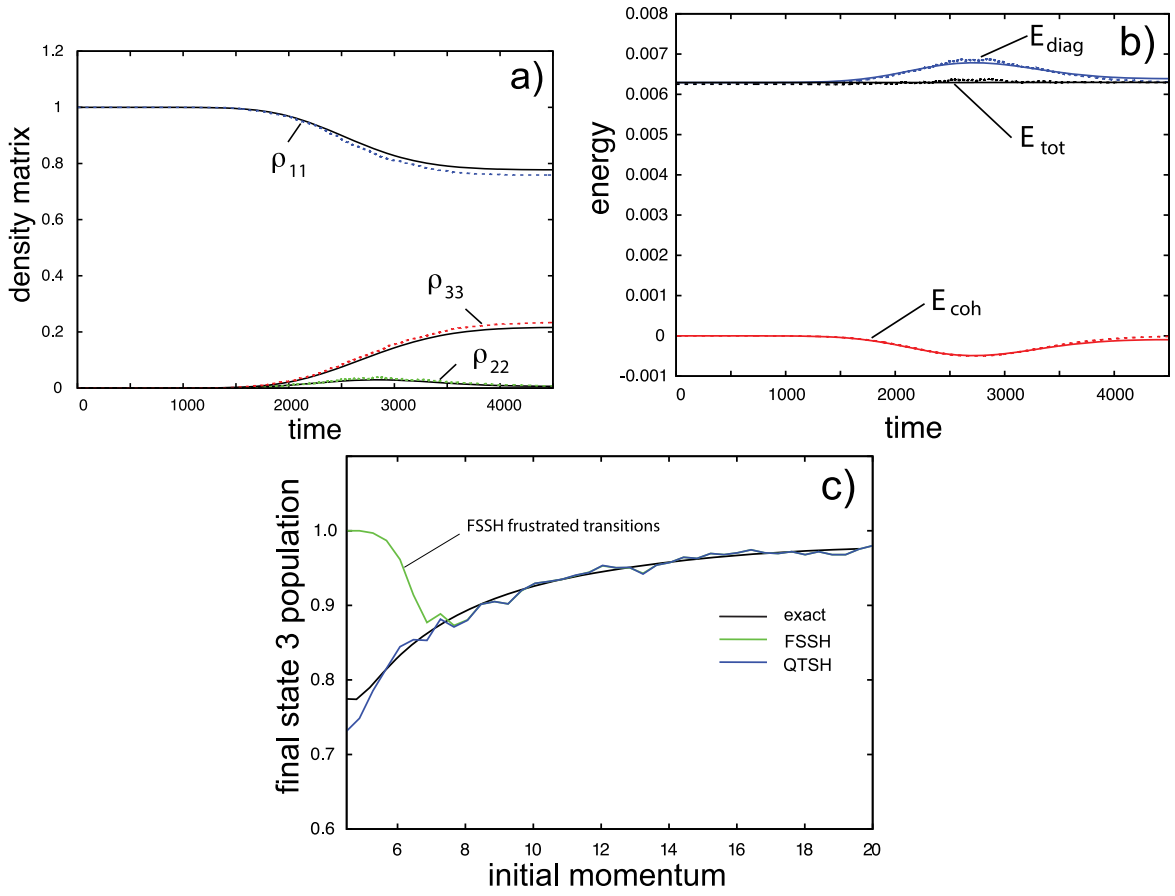

Figure 5. (a) Time dependence of the the state 1, 2, and 3 populations for the superexchange model. QTSH (solid) is compared with exact wavepacket results (dashed). Initial momentum $\hbar k = 5$. (b) The energy budget for the $\hbar k = 5$ ensemble. (c) Final state 3 population vs. initial momentum $\hbar k$. FSSH (green) and QTSH (blue) are compared with exact quantum results (black).

the QTSH and FSSH methods to calculate the population transfer. These results are compared with corresponding quantum-wavepacket results. All simulations are performed in the diabatic representation.

For $\hbar k \lesssim 6.3$, the mean kinetic energy of the state is insufficient to reach the intermediate state 2; the range of initial momenta between the minimum value to reach state 3 and this value is known as the superexchange region.

Figure 5a shows the state populations versus time for an initial state with momentum $\hbar k = 5$ within the superexchange region. The QTSH results are compared with exact quantum calculations. For this initial state, virtually all FSSH hops are frustrated, leading to no population transfer out of state 1 (results not shown). The QTSH populations are in nearly quantitative agreement with the quantum results for this classically forbidden process. Even the "virtual" state 2 populations are accurately represented by the ensemble of QTSH trajectories.

In Figure 5b, the QTSH energy budget for the state shown in panel a is presented and compared with the corresponding quantum-mechanical quantities. The total energy is well-conserved by the quantum trajectories. Again, we see that the diagonal energy is *not* conserved by the QTSH method or by the exact quantum evolution. This nonconservation is what allows the nonclassical superexchange mechanism to pass through state 2 and then populate the final state 3, and artificial imposition of energy conservation by FSSH is what leads to spuriously frustrated hops and the failure of that method.

In Figure 5c, the dependence of the final population of state 3 on the initial momentum $\hbar k$ is given. QTSH results are compared with FSSH and exact quantum simulations. For values of $k \gtrsim 7$, above the superexchange region, both QTSH and FSSH are in nearly exact agreement with the quantum results. As $\hbar k$ decreases into the classically forbidden superexchange region, the FSSH method fails to capture the population-transfer process, whereas QTSH remains in good agreement with the exact results.

In Figure 6, we demonstrate the time reversibility of the QTSH method. We consider the state treated in Figure 1 for the Tully single-crossing system in the adiabatic representation. Here we integrate the minimum uncertainty state with initial momentum $\hbar k = 10$ from $t = 0$ until an intermediate time $t = 2400$, for which the system has left the interaction region. The momentum, p_j, and imaginary part of the coherence, β_j, of each trajectory are then reversed in sign, and the ensemble is integrated to the final time of $t = 2 \times 2400 = 4800$. The figure shows the population of the initially occupied lower state as a function of time. The QTSH results are compared with the FSSH method. The QTSH method demonstrates nearly quantitative reversibility of the initial population, with only a slight asymmetry around the intermediate time $t = 2400$ and recovery of the full initial unit population to within statistical

DOI: 10.1021/acs.jpca.8b10487
J. Phys. Chem. A 2019, 123, 1110−1128

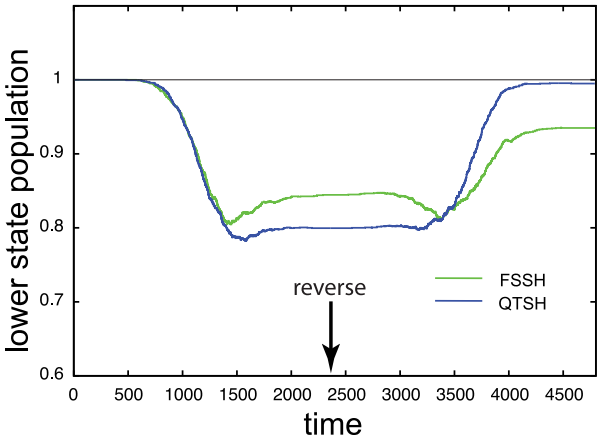

Figure 6. Time reversibility of surface-hopping methods. The time dependence of the adiabatic lower state population for Tully's single-crossing model in the adiabatic representation is shown for the FSSH (green) and QTSH (blue) methods for initial momentum $\hbar k = 10$. The simulation is run until $t = 2400$ (compare with Figure 1); then, the signs of the momenta, p_j, and imaginary part of the coherence, β_j, are reversed for each member of the ensemble, and the integration continued until $t = 4800$.

uncertainty. The FSSH method, on the contrary, demonstrates strong irreversibility resulting from the presence of frustrated hops and momentum rescaling of the trajectories.

In Figure 7, we investigate the efficacy of the ensemble-level decoherence correction described in the last section. Figure 7a compares the decoherence-corrected QTSH results with the uncorrected QTSH and exact quantum results, reproduced from Figure 1a. The incorporation of the decoherence factor $\chi(t)$ into the hopping probability brings the long-time lower state probability into close agreement with the quantum results, although the full time-dependent populations are not superimposable. In Figure 7b, we show the time dependence of the proxy phase variance $\delta\phi^2(t) = \langle\phi^2(t)\rangle - \langle\phi(t)\rangle^2$ and the global decoherence factor $\chi(t) = \exp(-\delta\phi^2(t)/2)$ for the ensemble describing the state in Figure 7a. The effect of phase dispersion across the ensemble is apparent, with significant variance of the trajectory phases during the hopping process. This results in the value of χ dropping from the fully coherent value of 1.0 to ~0.5 during the transition period. Importantly, though, it is observed that the ensemble recoheres to nearly full coherence by the end of the evolution. This is a characteristic of the underlying pure-state evolution of the system. Alternate methods for decoherence correction that irreversibly cause a decay of the trajectory coherence will miss this important feature of the ensemble dynamics.

4. CONCLUSIONS

We reviewed the CSH approach, introduced in a recent publication.[12] In addition, we significantly extended the formalism to include nonclassical state-dependent forces that take the place of the physically sensible but ad hoc momentum rescaling and resulting strict classical energy conservation of the FSSH method. The result is a quantum-trajectory -based formalism for simulating molecular dynamics with electronic transitions, where the quantum and classical portions of the mixed quantum-classical system are correctly entangled with each other.

The CSH method is based solidly on a solution of the underlying quantum Liouville equation in a mixed quantum-classical approximation using an ensemble of trajectories. A key aspect of the approach is that the trajectories in the ensemble are no longer independent, but their evolution is mutually coupled by their role in propagating the phase-space representation of the full quantum-classical density matrix. Quantum coherence emerges naturally as a characteristic of the ensemble as a whole via the interrelationships between individual trajectory phases. Decoherence is captured by the method without externally imposed corrections.

Despite these formal advantages, the CSH method is too intensive numerically to be a practical method for anything beyond simple model systems. To address this shortcoming, we have introduced further well-defined approximations to the CSH approach to derive an independent trajectory limit of the theory, which we call QTSH. This method recovers the fewest-switches stochastic algorithm for independent trajectories

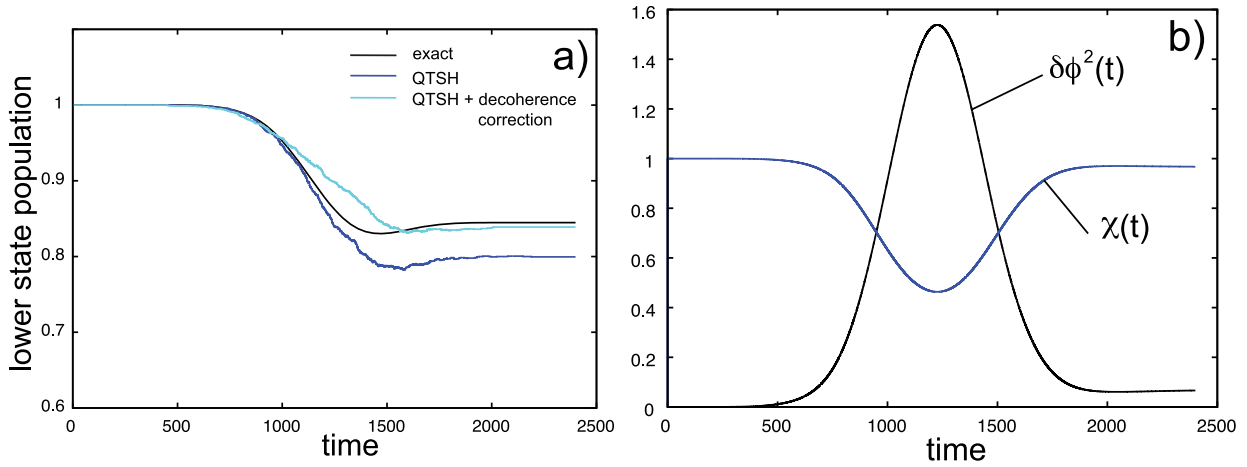

Figure 7. Ensemble-level coherence correction. (a) Time dependence of the adiabatic lower state population for Tully's single-crossing model. Exact wavepacket calculations (black) are compared with both the unmodified QTSH (blue) and QTSH + ensemble-level decoherence-corrected (cyan) results for initial momentum of $\hbar k = 30$. Calculations are done in the adiabatic representation. (b) Time dependence of the phase variance $\delta\phi^2(t)$ and decoherence factor $\chi(t)$ for the QTSH ensemble in panel a.

DOI: 10.1021/acs.jpca.8b10487
J. Phys. Chem. A 2019, 123, 1110−1128

employed in FSSH. However, the momentum rescaling and classical trajectory energy conservation of FSSH are discarded in favor of the rigorously derived quantum forces of the CSH formalism. The cost of QTSH is comparable to that of FSSH. We illustrated the QTSH methodology by treating several simple model systems commonly used as benchmarks for surface-hopping approaches.

QTSH rigorously conserves the correct quantum-classical energy $\mathrm{Tr}(H\rho)$ without ad hoc momentum rescaling. This is due to the presence of the nonclassical forces in the quantum trajectory evolution. Energy conservation results without any artificial momentum rescaling, eliminating undesirable features of FSSH such as forbidden hops and the breakdown of the internal consistency of quantum- and ensemble-based state probabilities. In the adiabatic representation, the classical dynamics are modified by a quantum-state-dependent vector potential, introducing geometric phase effects into the dynamics for multidimensional systems. Another advantage of the QTSH method is that it is time-reversible at the ensemble level, unlike FSSH, where frustrated hops and momentum rescaling break the time-reversal symmetry of even pure-state quantum evolution. We have proposed further approximate corrections inspired by the underlying CSH formalism that allow the incorporation of ensemble-level decoherence without the accompanying computational expense of CSH.

The present manuscript has mainly focused on the formal development of the CSH and QTSH approaches. Detailed numerical investigations and extensions to higher dimensional systems and realistic applications, including geometric phase effects resulting from the nonclassical forces in the adiabatic representation, will be presented in future publications.

The surface-hopping approach to simulating molecular dynamics in the quantum-classical limit is just one example of a "quantum trajectory" formalism. Methods that treat quantum-mechanical processes with trajectory ensembles are effectively hidden variable theories, where the evolving quantum state, wave function, ψ, or density operator, $\hat{\rho}$, depends on hidden parameters that are not themselves immediately accessible to scrutiny.[53−56] In the quantum trajectory case, these variables are the unobservable positions and momenta of the individual trajectories comprising the ensemble representing the quantum state.

In the classical limit, the relationship between a single trajectory and a statistical ensemble of independent trajectories is a familiar example of a local hidden variable theory, where each trajectory has a well-defined and independent motion, representing a "real" realization of the statistical state. In classical mechanics there are no problems, such as entanglement, nonlocality, or the uncertainty principle, preventing the arbitrarily fine dissection of the phase-space probability distribution into its constituent trajectories and considering them as independent deterministic time histories. In quantum systems, however, Bell's theorem shows quite generally that no local hidden variable theory is compatible with quantum mechanics.[55,57] In a quantum trajectory context, this leads to nonclassical trajectory dynamics that cannot be treated independently from the quantum state itself, or, equivalently, from the full trajectory ensemble. Bohm's original causal theory is the earliest nonlocal theory, where the system wave function leads to a quantum force that guides trajectories.[58,59] Examples of methods based on nonlocal hidden variable theories in chemical physics include Bohmian dynamics,[60−62] many interacting worlds formalism,[63,64] and our work on quantum tunneling using entangled trajectories.[32,34,65,66]

In the surface-hopping context, the independent trajectory basis of both FSSH and QTSH leads them to be local hidden variable theories. As such, although they may be accurate for many problems in practice, they cannot, in principle, give exact agreement with quantum mechanics generally. CSH, on the contrary, is an example of a nonlocal hidden variable theory. Future work will focus on developing the CSH framework into an exact trajectory representation of nonadiabatic processes, not as a practical method, but as a context in which to understand fundamental aspects of quantum theory.

AUTHOR INFORMATION

Corresponding Author

*E-mail: cmartens@uci.edu.

ORCID

Craig C. Martens: 0000-0002-2350-4346

Notes

The author declares no competing financial interest.

ACKNOWLEDGMENTS

We are grateful to Shaul Mukamel, Vladimir Mandelshtam, and Filipp Furche for helpful conversations. Stimulating discussions at the UCI Liquid Theory Lunch (LTL) and the Telluride Science Research Center (TSRC) are also acknowledged. This material is based on work supported by the National Science Foundation under CHE-1764209.

REFERENCES

(1) Tully, J. C. Molecular Dynamics with Electronic Transitions. *J. Chem. Phys.* **1990**, *93*, 1061.

(2) Tully, J. C. Perspective: Nonadiabatic Dynamics Theory. *J. Chem. Phys.* **2012**, *137*, 22A301.

(3) Subotnik, J. E.; Shenvi, N. A New Approach to Decoherence and Momentum Rescaling in the Surface Hopping Algorithm. *J. Chem. Phys.* **2011**, *134*, 024105.

(4) Jaeger, H. M.; Fischer, S.; Prezhdo, O. V. Decoherence-Induced Surface Hopping. *J. Chem. Phys.* **2012**, *137*, 22A545.

(5) Subotnik, J. E.; Ouyang, W.; Landry, B. R. Can We Derive Tully's Surface-Hopping Algorithm from the Semiclassical Quantum Liouville Equation? Almost, But Only with Decoherence. *J. Chem. Phys.* **2013**, *139*, 214107.

(6) Curchod, B. F. E.; Tavernelli, I. On Trajectory-Based Nonadiabatic Dynamics: Bohmian Dynamics versus Trajectory Surface Hopping. *J. Chem. Phys.* **2013**, *138*, 184112.

(7) Belyaev, A. K.; Lasser, C.; Trigila, G. Landau−Zener Type Surface Hopping Algorithms. *J. Chem. Phys.* **2014**, *140*, 224108.

(8) Chen, H.-T.; Reichman, D. R. On the Accuracy of Surface Hopping Dynamics in Condensed Phase Non-Adiabatic Problems. *J. Chem. Phys.* **2016**, *144*, 094104−10.

(9) Wang, L.; Akimov, A.; Prezhdo, O. V. Recent Progress in Surface Hopping: 2011−2015. *J. Phys. Chem. Lett.* **2016**, *7*, 2100−2112.

(10) Subotnik, J. E.; Jain, A.; Landry, B.; Petit, A.; Ouyang, W.; Bellonzi, N. Understanding the Surface Hopping View of Electronic Transitions and Decoherence. *Annu. Rev. Phys. Chem.* **2016**, *67*, 387−417.

(11) Crespo-Otero, R.; Barbatti, M. Recent Advances and Perspectives on Nonadiabatic Mixed Quantum−Classical Dynamics. *Chem. Rev.* **2018**, *118*, 7026−7068.

(12) Martens, C. C. Surface Hopping by Consensus. *J. Phys. Chem. Lett.* **2016**, *7*, 2610−2615.

(13) Martens, C. C. Nonadiabatic Dynamics in the Semiclassical Liouville Representation: Locality, Transformation Theory, and the Energy Budget. *Chem. Phys.* **2016**, *481*, 60−68.

DOI: 10.1021/acs.jpca.8b10487
J. Phys. Chem. A 2019, 123, 1110−1128

(14) Martens, C. C.; Fang, J. Y. Semiclassical-Limit Molecular Dynamics on Multiple Electronic Surfaces. *J. Chem. Phys.* **1997**, *106*, 4918−4930.
(15) Donoso, A.; Martens, C. C. Simulation of Coherent Nonadiabatic Dynamics Using Classical Trajectories. *J. Phys. Chem. A* **1998**, *102*, 4291−4300.
(16) Donoso, A.; Martens, C. C. Semiclassical Multi-State Liouville Dynamics in the Adiabatic Representation. *J. Chem. Phys.* **2000**, *112*, 3980−3989.
(17) Donoso, A.; Kohen, D.; Martens, C. C. Simulation of Nonadiabatic Wavepacket Interferometry Using Classical Trajectories. *J. Chem. Phys.* **2000**, *112*, 7345−7354.
(18) Donoso, A.; Martens, C. C. Classical Trajectory-Based Approaches to Solving the Quantum Liouville Equation. *Int. J. Quantum Chem.* **2002**, *90*, 1348−1360.
(19) Kapral, R.; Ciccotti, G. Mixed Quantum-Classical Dynamics. *J. Chem. Phys.* **1999**, *110*, 8919.
(20) Nielsen, S.; Kapral, R.; Ciccotti, G. Mixed Quantum-Classical Surface Hopping Dynamics. *J. Chem. Phys.* **2000**, *112*, 6543.
(21) Cohen-Tannoudji, C.; Diu, B.; Laloe, F. *Quantum Mechanics*; Wiley: New York, 1977.
(22) McQuarrie, D. A. *Statistical Mechanics*; HarperCollins: New York, 1976.
(23) Takahashi, K. Distribution Functions in Classical and Quantum Mechanics. *Prog. Theor. Phys. Suppl.* **1989**, *98*, 109−156.
(24) Mukamel, S. *Principles of Nonlinear Optical Spectroscopy*; Oxford University Press: Oxford, U.K., 1995.
(25) Riga, J. M.; Martens, C. C. Simulation of Environmental Effects on Coherent Quantum Dynamics in Many-Body Systems. *J. Chem. Phys.* **2004**, *120*, 6863−6873.
(26) Riga, J. M.; Fredj, E.; Martens, C. C. Quantum Vibrational State-Dependent Potentials for Classical Many-Body Simulations. *J. Chem. Phys.* **2005**, *122*, 174107.
(27) Riga, J. M.; Martens, C. C. Environmental Decoherence of Many-Body Quantum Systems: Semiclassical Theory and Simulation. *Chem. Phys.* **2006**, *322*, 108−117.
(28) Riga, J.; Fredj, E.; Martens, C. Simulation of Vibrational Dephasing of I_2 in solid Kr Using the Semiclassical Liouville Method. *J. Chem. Phys.* **2006**, *124*, 064506.
(29) Hogan, P. A.; Fredj, E.; Martens, C. C. Simulation of Vibrational Dephasing in Liquid Water Using the Semiclassical Liouville Method. *Chem. Phys. Lett.* **2011**, *510*, 208−211.
(30) Roman, E.; Martens, C. C. Semiclassical Liouville Method for the Simulation of Electronic Transitions: Single Ensemble Formulation. *J. Chem. Phys.* **2004**, *121*, 11572.
(31) Martens, C. C. Communication: Fully Coherent Quantum State Hopping. *J. Chem. Phys.* **2015**, *143*, 141101.
(32) Donoso, A.; Martens, C. C. Quantum Tunneling Using Entangled Classical Trajectories. *Phys. Rev. Lett.* **2001**, *87*, 223202.
(33) Donoso, A.; Martens, C. C. Solution of Phase Space Diffusion Equations Using Interacting Trajectory Ensembles. *J. Chem. Phys.* **2002**, *116*, 10598.
(34) Donoso, A.; Zheng, Y.; Martens, C. C. Simulation of Quantum Processes Using Entangled trajectory molecular dynamics. *J. Chem. Phys.* **2003**, *119*, 5010.
(35) Hogan, P.; Van Wart, A.; Donoso, A.; Martens, C. C. Solving Evolution Equations Using Interacting Trajectory Ensembles. *Chem. Phys.* **2010**, *370*, 20.
(36) Meyer, H. D.; Miller, W. H. A Classical Analog for Electronic Degrees of Freedom in Nonadiabatic Collision Processes. *J. Chem. Phys.* **1979**, *70*, 3214.
(37) Cotton, S. J.; Miller, W. H. Symmetrical Windowing for Quantum States in Quasi-Classical Trajectory Simulations: Application to Electronically Non-Adiabatic Processes. *J. Chem. Phys.* **2013**, *139*, 234112.
(38) Cotton, S. J.; Liang, R.; Miller, W. H. On the Adiabatic Representation of Meyer-Miller Electronic-Nuclear Dynamics. *J. Chem. Phys.* **2017**, *147*, 064112−11.
(39) Tao, G. A Multi-State Trajectory Method for Non-Adiabatic Dynamics Simulations. *J. Chem. Phys.* **2016**, *144*, 094108−9.
(40) Tao, G. Multi-State Trajectory Approach to Non-Adiabatic Dynamics: General Formalism and the Active State Trajectory Approximation. *J. Chem. Phys.* **2017**, *147*, 044107−12.
(41) Ando, K. Non-Adiabatic Couplings in Liouville Description of Mixed Quantum-Classical Dynamics. *Chem. Phys. Lett.* **2002**, *360*, 240−242.
(42) Ando, K.; Santer, M. Mixed Quantum-Classical Liouville Molecular Dynamics without Momentum Jump. *J. Chem. Phys.* **2003**, *118*, 10399−10406.
(43) Ryabinkin, I. G.; Hsieh, C.-Y.; Kapral, R.; Izmaylov, A. F. Analysis of Geometric Phase Effects in the Quantum-Classical Liouville Formalism. *J. Chem. Phys.* **2014**, *140*, 084104.
(44) Ryabinkin, I. G.; Joubert-Doriol, L.; Izmaylov, A. F. When Do We Need to Account for the Geometric Phase in Excited State Dynamics? *J. Chem. Phys.* **2014**, *140*, 214116−12.
(45) Ryabinkin, I. G.; Joubert-Doriol, L.; Izmaylov, A. F. Geometric Phase Effects in Nonadiabatic Dynamics near Conical Intersections. *Acc. Chem. Res.* **2017**, *50*, 1785−1793.
(46) Xie, C.; Kendrick, B. K.; Yarkony, D. R.; Guo, H. Constructive and Destructive Interference in Nonadiabatic Tunneling via Conical Intersections. *J. Chem. Theory Comput.* **2017**, *13*, 1902−1910.
(47) Kendrick, B. K.; Hazra, J.; Balakrishnan, N. The Geometric Phase Controls Ultracold Chemistry. *Nat. Commun.* **2015**, *6*, 7918−7.
(48) Parandekar, P. V.; Tully, J. C. Detailed Balance in Ehrenfest Mixed Quantum-Classical Dynamics. *J. Chem. Theory Comput.* **2006**, *2*, 229−235.
(49) Jain, A.; Subotnik, J. E. Surface Hopping, Transition State Theory, and Decoherence. II. Thermal Rate Constants and Detailed Balance. *J. Chem. Phys.* **2015**, *143*, 134107−14.
(50) Sifain, A. E.; Wang, L.; Prezhdo, O. V. Communication: Proper Treatment of Classically Forbidden Electronic Transitions Significantly Improves Detailed Balance in Surface Hopping. *J. Chem. Phys.* **2016**, *144*, 211102−6.
(51) Kosloff, R. Propagation Methods for Quantum Molecular Dynamics. *Annu. Rev. Phys. Chem.* **1994**, *45*, 145.
(52) Wang, L.; Trivedi, D.; Prezhdo, O. V. Global Flux Surface Hopping Approach for Mixed Quantum-Classical Dynamics. *J. Chem. Theory Comput.* **2014**, *10*, 3598−3605.
(53) Jammer, M. *The Philosophy of Quantum Mechanics*; Wiley: New York, 1974.
(54) *Quantum Theory and Measurement*; Zurek, W. H., Wheeler, J. A., Eds.; Princeton University Press: Princeton, NJ, 1983.
(55) Bell, J. S. *Speakable and Unspeakable in Quantum Mechanics*; Cambridge University Press: Cambridge, U.K., 1987.
(56) Selleri, F. *Quantum Paradoxes and Physical Reality*; Kluwer Academic: Dordrecht, The Netherlands, 1990.
(57) Bell, J. S. On the Problem of Hidden Variables in Quantum Mechanics. *Rev. Mod. Phys.* **1966**, *38*, 447−452.
(58) Bohm, D. A Suggested Interpretation of the Quantum Theory in Terms of Hidden Variables 0.1. *Phys. Rev.* **1952**, *85*, 166−179.
(59) Holland, P. R. *The Quantum Theory of Motion*; Cambridge University Press: Cambridge, U.K., 1995.
(60) Dey, B. K.; Askar, A.; Rabitz, H. Multidimensional Wave Packet Dynamics within the Fluid Dynamical Formulation of the Schrodinger Equation. *J. Chem. Phys.* **1998**, *109*, 8770−8782.
(61) Lopreore, C. L.; Wyatt, R. E. Quantum Wave Packet Dynamics with Trajectories. *Phys. Rev. Lett.* **1999**, *82*, 5190−5193.
(62) Wyatt, R. *Quantum Dynamics with Trajectories: Introduction to Quantum Hydrodynamics*; Springer: New York, 2005.
(63) Schiff, J.; Poirier, B. Communication: Quantum Mechanics Without Wavefunctions. *J. Chem. Phys.* **2012**, *136*, 031102.
(64) Hall, M. J. W.; Deckert, D.-A.; Wiseman, H. M. Quantum Phenomena Modeled by Interactions between Many Classical Worlds. *Phys. Rev. X* **2014**, *4*, 041013−17.
(65) Wang, A.; Zheng, Y.; Ren, W.; Martens, C. C. Quantum Dynamics using Entangled Trajectories: General Potentials. *Phys. Chem. Chem. Phys.* **2009**, *11*, 1588.

DOI: 10.1021/acs.jpca.8b10487
J. Phys. Chem. A 2019, 123, 1110−1128

(66) Wang, L.; Martens, C. C.; Zheng, Y. Entangled Trajectory Molecular Dynamics in Multidimensional Systems: Two-Dimensional Quantum Tunneling Through the Eckart Barrier. *J. Chem. Phys.* **2012**, *137*, 034113.

DOI: 10.1021/acs.jpca.8b10487
J. Phys. Chem. A 2019, 123, 1110−1128